



Planck dust polarization measurements

and contamination on the BICEP2 gravitational waves result

Francesco Piacentini

University of Roma “La Sapienza”
Planck HFI Collaboration

francesco.piacentini@roma1.infn.it

November 25, 2014

March 2014 – breaking news

- The BICEP2 team claimed the first measure of:
 - The B-mode of the cosmic microwave background (CMB) polarization
 - Measured at a spectacularly high level
 $r = 0.2^{+0.07}_{-0.05}$
 - This should be caused by gravitational waves presents at the time the CMB is last scattered (380'000 year after Big Bang)
 - Measured with the South Pole based, microwave sensitive telescope

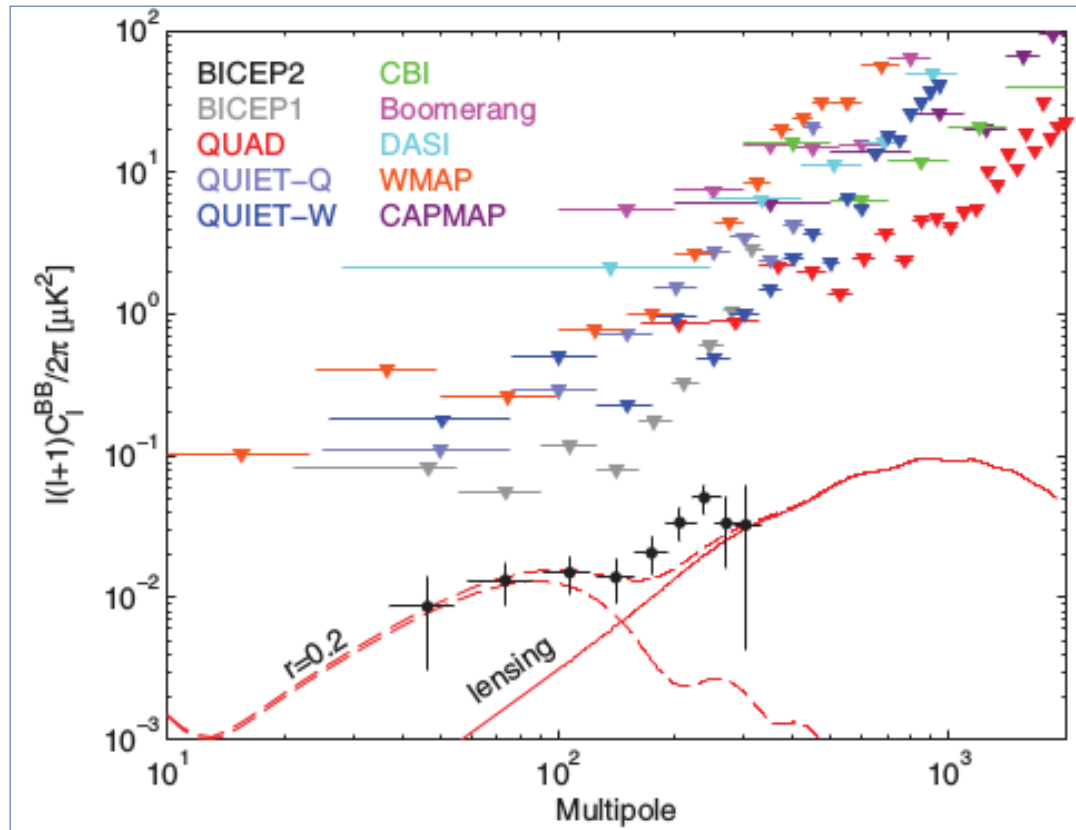


FIG. 14 (color). BICEP2 BB auto spectra and 95% upper limits from several previous experiments [2,40,42,43,47,49–51,107]. The curves show the theory expectations for $r = 0.2$ and lensed Λ CDM. The BICEP2 uncertainties include sample variance on an $r = 0.2$ contribution.

March 2014 – breaking news

- What BICEP2 measured:
 - The statistical fluctuation of the CMB polarization
 - In particular, a component which presents a vortex pattern (**B-modes**)
 - In the early Universe, only **Gravitational Waves** could have created such pattern in the CMB polarization

- A similar pattern can be generated by polarized emission of dust in our Galaxy
- BICEP2 had no good data to constrain dust contamination
- Planck is now providing these data

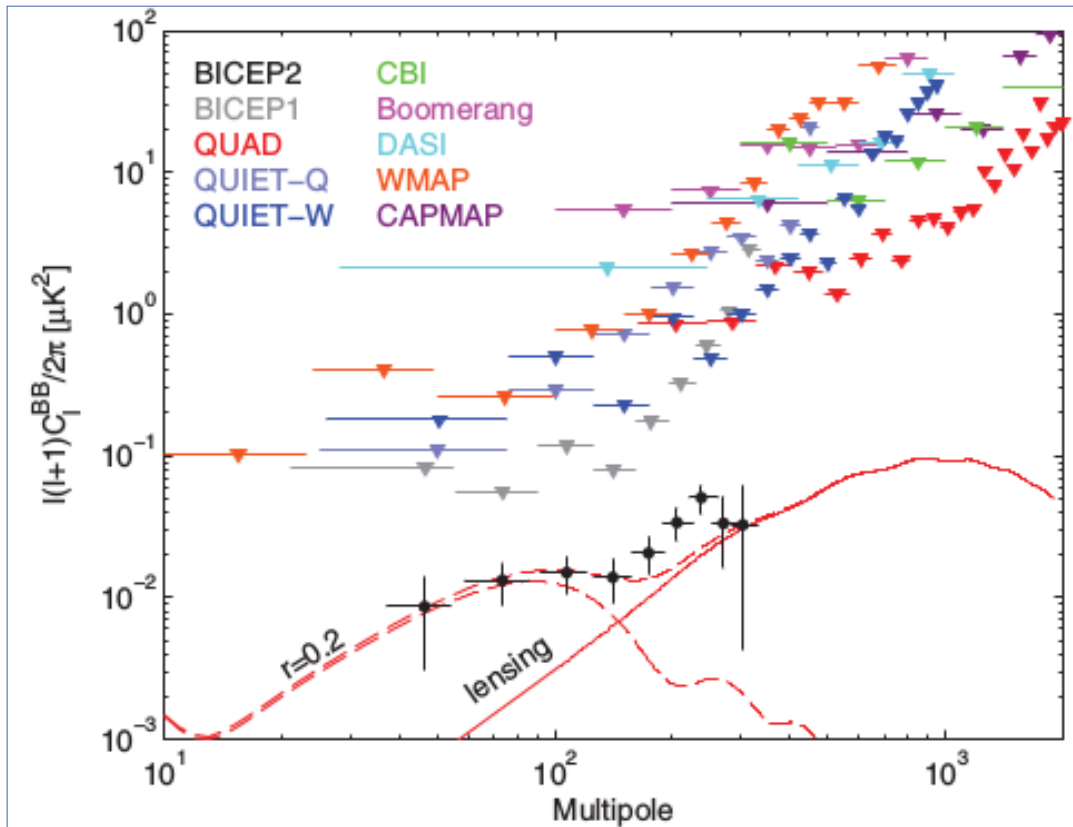
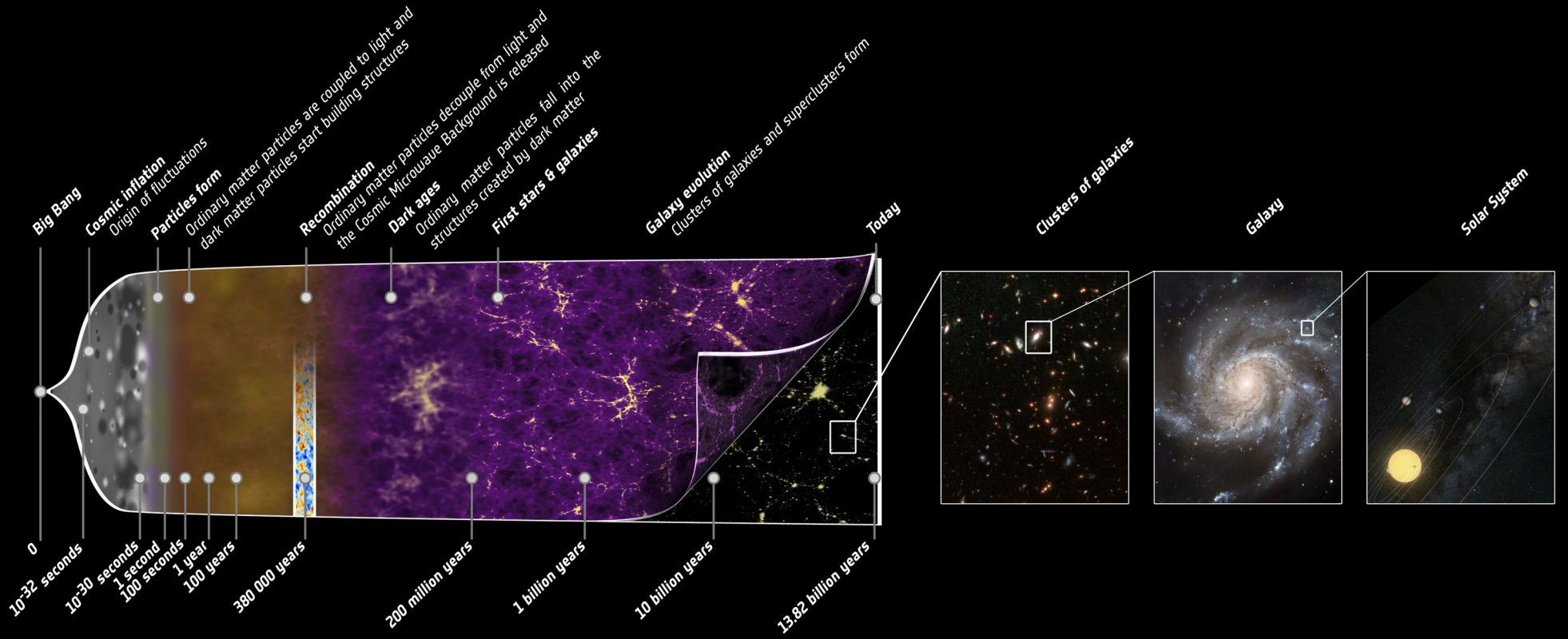


FIG. 14 (color). BICEP2 *BB* auto spectra and 95% upper limits from several previous experiments [2,40,42,43,47,49–51,107]. The curves show the theory expectations for $r = 0.2$ and lensed Λ CDM. The BICEP2 uncertainties include sample variance on an $r = 0.2$ contribution.



CMB polarization review

History of the Universe



Inflation epoch
Plasma epoch
Last Scattering

Plasma in the early Universe

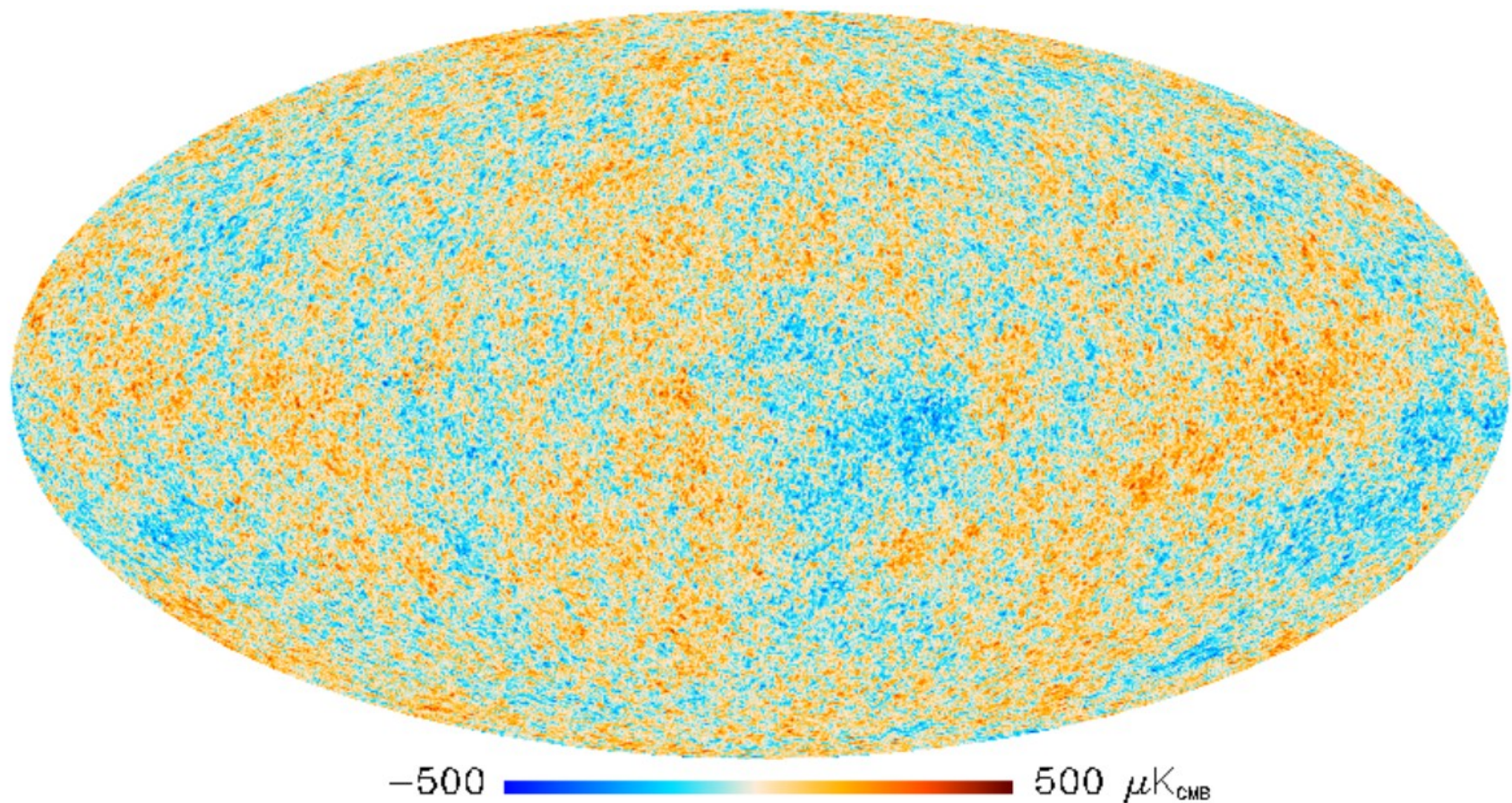
- Before 380'000 year after Big Bang, the Universe is filled with
 - Hydrogen (and Helium) plasma + Photons
 - Coupled by Thomson scattering
 - Oscillating by effect of gravity and (radiation) pressure

- Recombination
 - At 380'000 year, the plasma recombine and the photons mean free path become longer than the Universe scale:
 - the Universe becomes transparent
 - Matter and radiation decouple

 - The oscillations are imprinted into the CMB when primordial plasma recombine
 - Synchronized by the fact that all perturbations at a given scale (\mathbf{k}) start oscillating at the same time
 - Oscillation starts when the perturbation with wavelength λ ($=2\pi/k$) enters the causal horizon ($\lambda \sim ct$)
 - This process leave a 1 degree characteristics scale in the CMB image

CMB temperature fluctuations

- Planck 2013 map, after subtraction of:
 - Monopole (2.726 Kelvin)
 - Dipole (3.346 mK)
 - Milky Way emission



Angular power spectrum

- Decomposition in spherical harmonics

$$T(\theta, \phi) = \sum_{\ell=0}^{\infty} \sum_{m=-\ell}^{\ell} a_{\ell m} Y_{\ell m}(\theta, \phi)$$

$$\langle a_{\ell m} \rangle = 0$$

- Variance of the spherical harmonic coefficients (assuming no preferred direction)

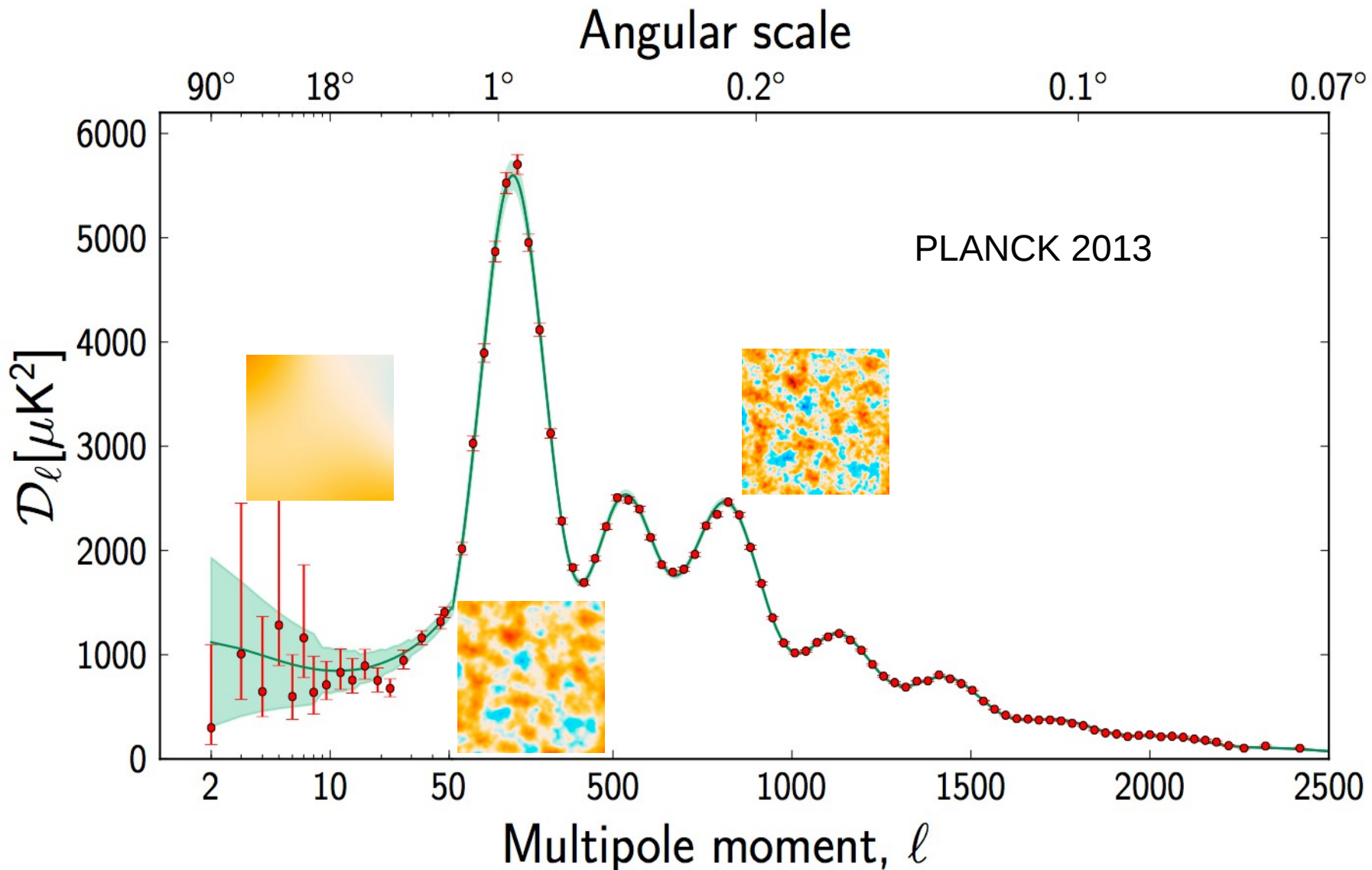
$$\langle |a_{\ell m}|^2 \rangle \neq 0$$

$$\langle |a_{\ell,m}|^2 \rangle = C_\ell$$

$$D_\ell = \frac{\ell(\ell+1)}{2\pi} \langle |a_{\ell m}|^2 \rangle$$

Angular power spectrum

- Comparing data and model, cosmologists measure parameters



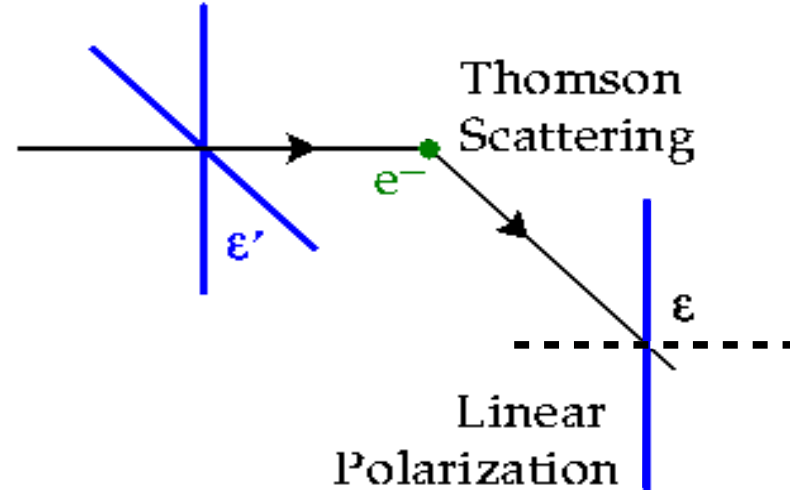
CMB polarization

- Before 380'000 year after Big Bang, the Universe is filled with
 - Hydrogen and Helium plasma
 - Photons
 - Coupled by Thomson scattering

CMB polarization

- Thomson scattering can polarize radiation

$$\frac{d\sigma}{d\Omega} = \frac{3\sigma_T}{8\pi} |\hat{\epsilon} \cdot \hat{\epsilon}'|^2$$

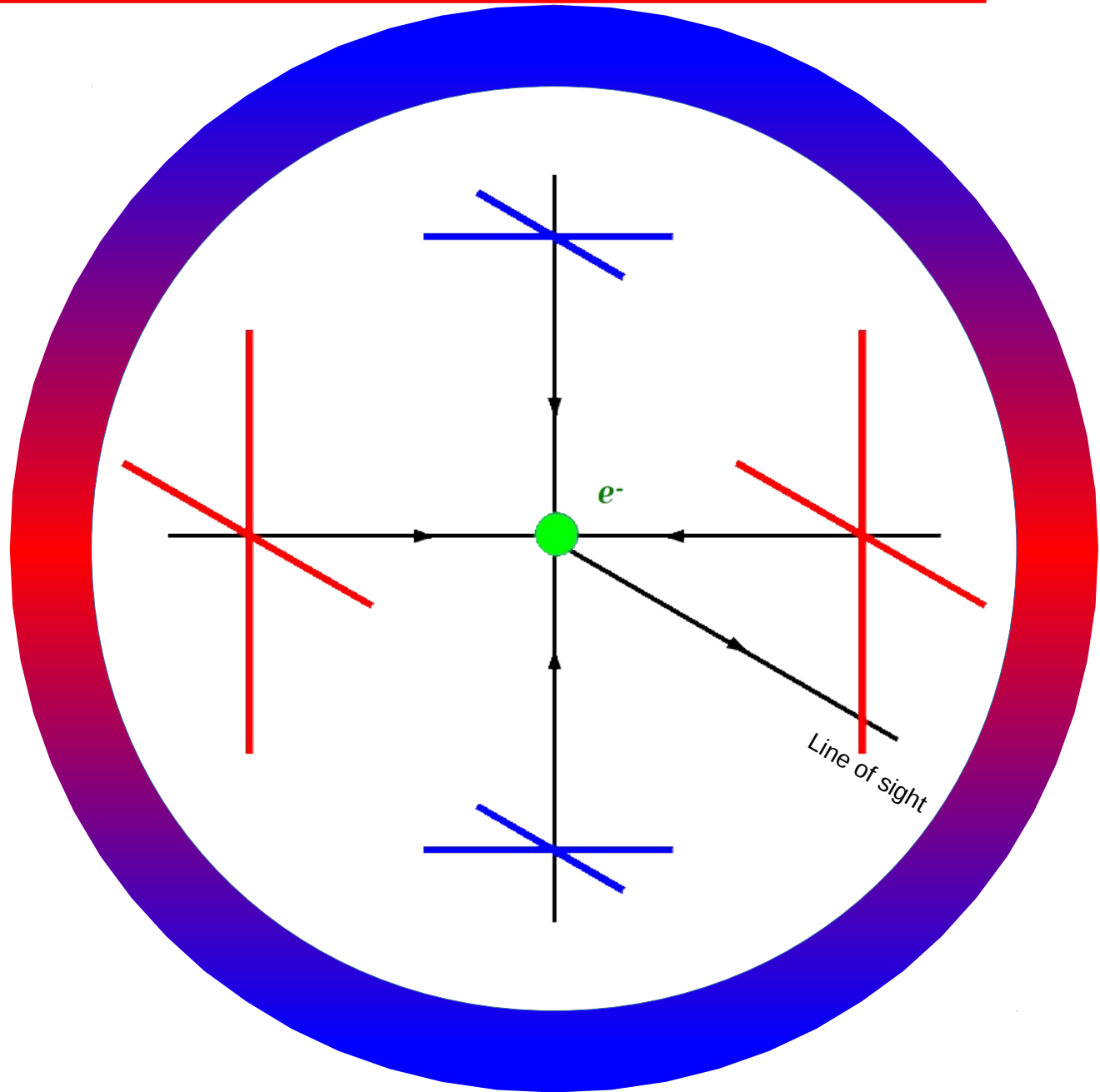


CMB polarization

- Thomson scattering can polarize radiation

$$\frac{d\sigma}{d\Omega} = \frac{3\sigma_T}{8\pi} |\hat{\epsilon} \cdot \hat{\epsilon}'|^2$$

- Incoming radiation must have quadrupolar asymmetry

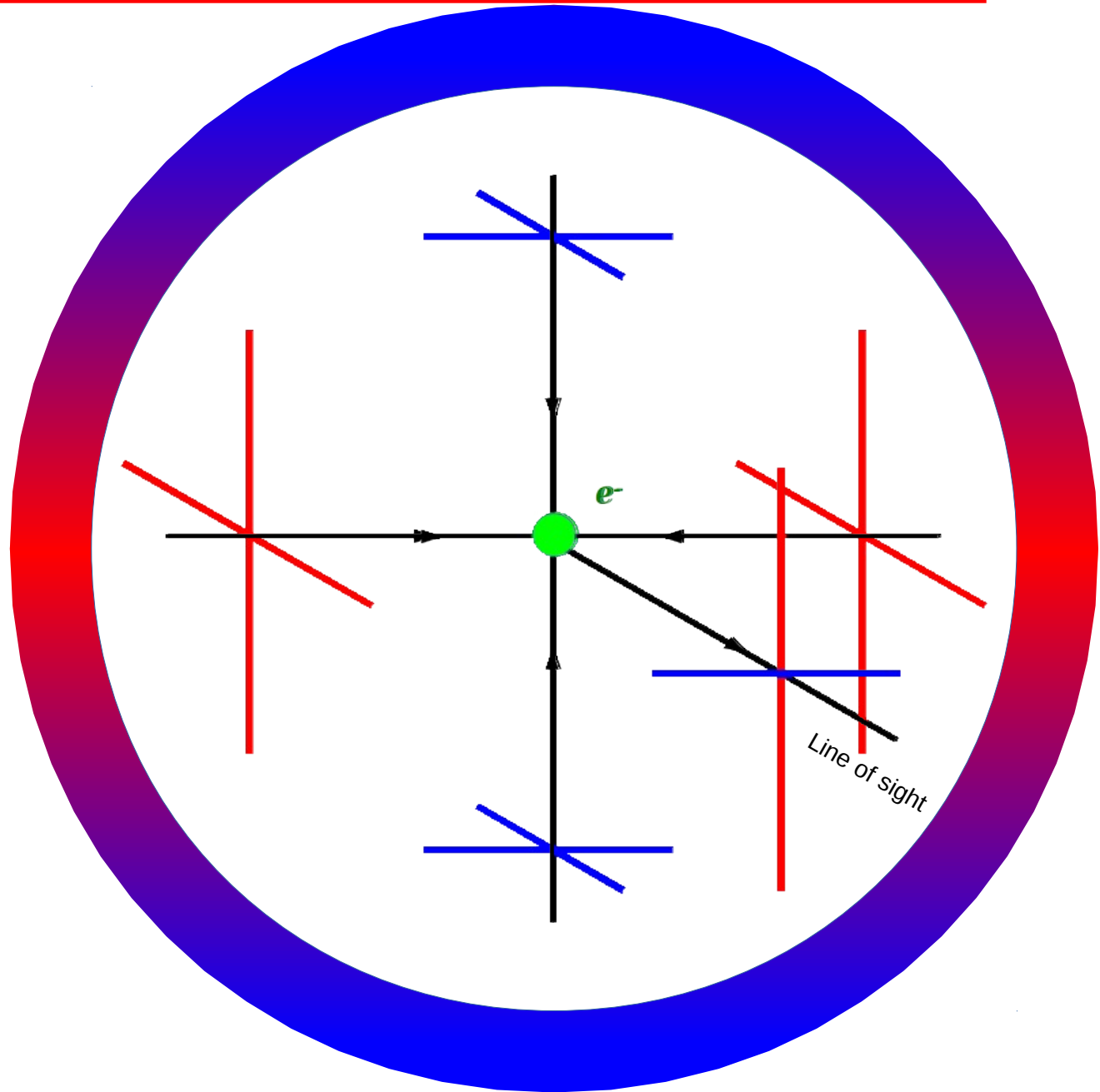


CMB polarization

- Thomson scattering can polarize radiation

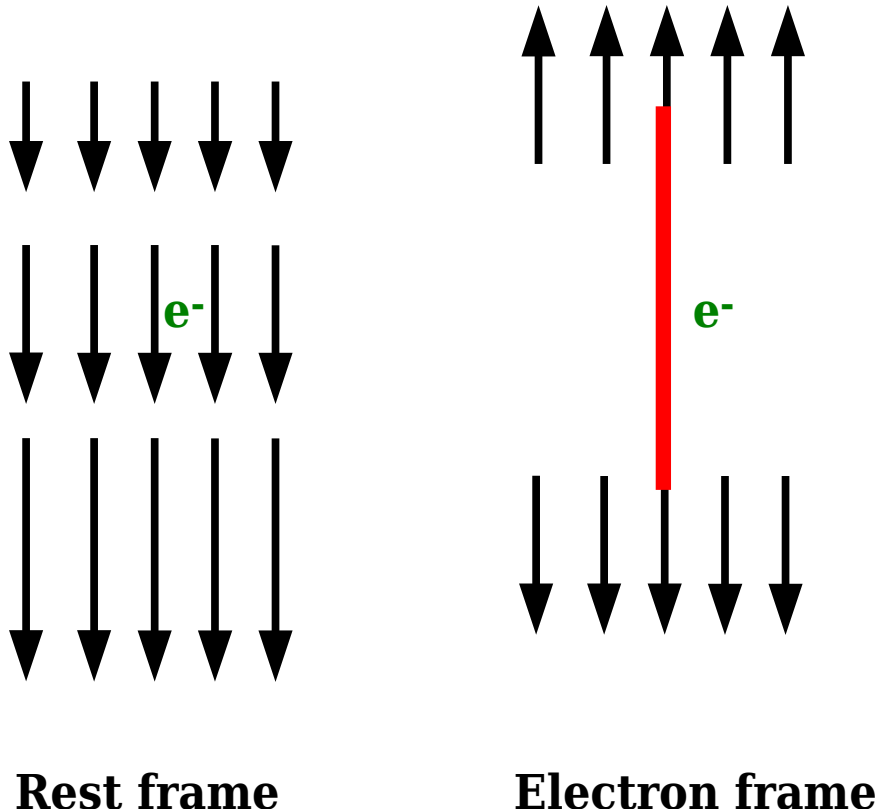
$$\frac{d\sigma}{d\Omega} = \frac{3\sigma_T}{8\pi} |\hat{\epsilon} \cdot \hat{\epsilon}'|^2$$

- Incoming radiation must have quadrupolar asymmetry

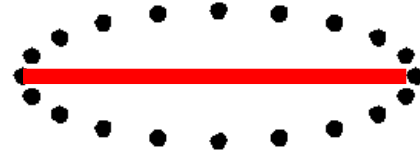


CMB polarization

- Plasma accelerated flows generate quadrupolar asymmetry via Doppler effect



- Gravitational waves stretch space, causing red-shift and blue-shift

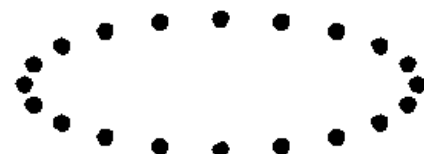


Gravitational waves

- From general relativity
 - distance between two points in space, first order approximation

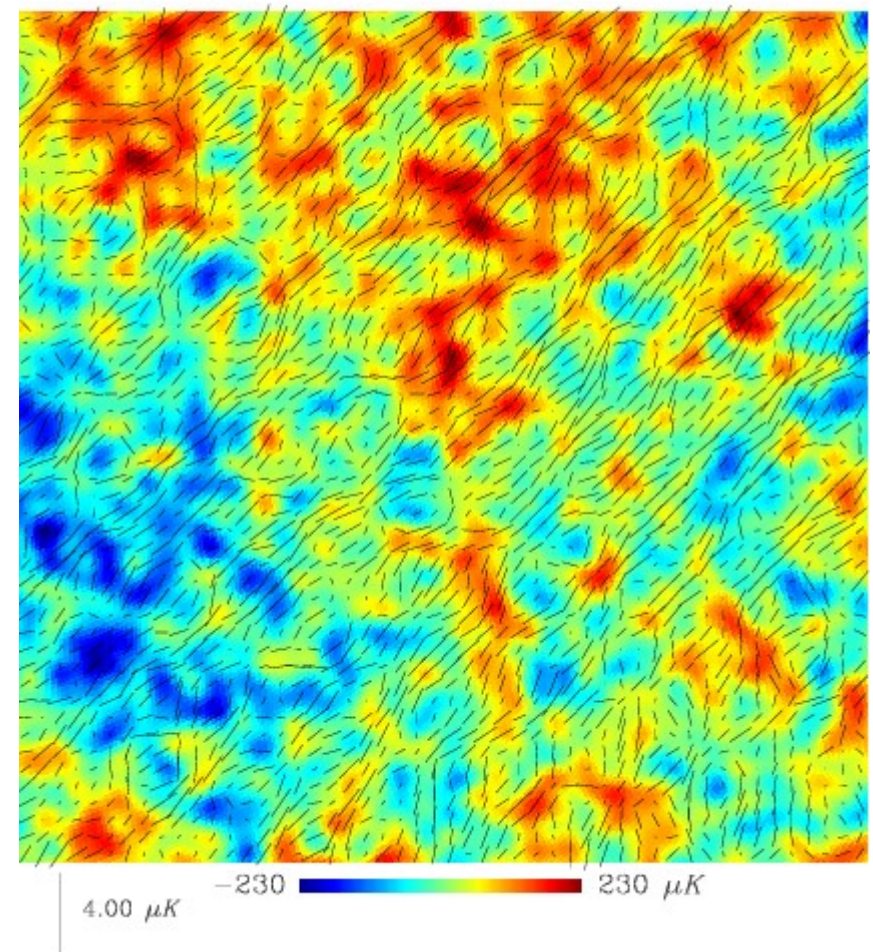
$$dl^2 = a^2(t)[1 + 2\zeta(x, t) + \dots][\delta_{ij} + h_{ij}(x, t) + \dots]dx^i dx^j$$

- $\zeta(x, t)$ = curvature perturbation (scalar mode)
- $h(x, t)$ = gravitational wave (tensor mode)
 - anisotropic stretching of space, with conservation of area



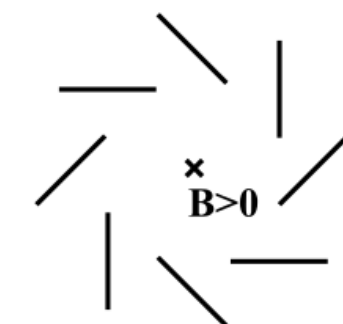
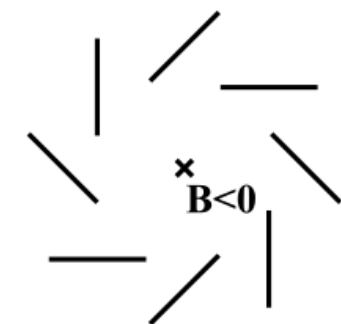
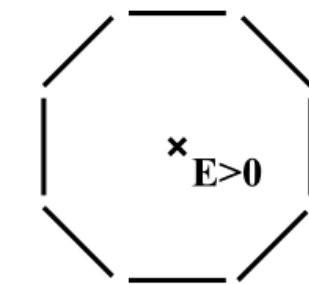
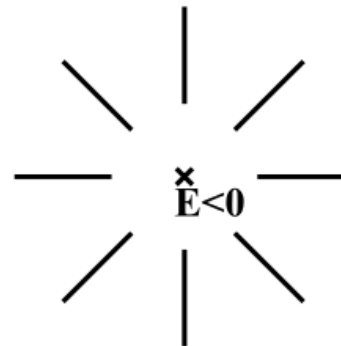
Intensity and polarization map

- Intensity (color)
- Q, U Stokes parameters (rods)
 - Q, U depend on the reference frame
 - Q, U are spin-2 quantities:
 - Rotation by 180 deg = identity



CMB polarization

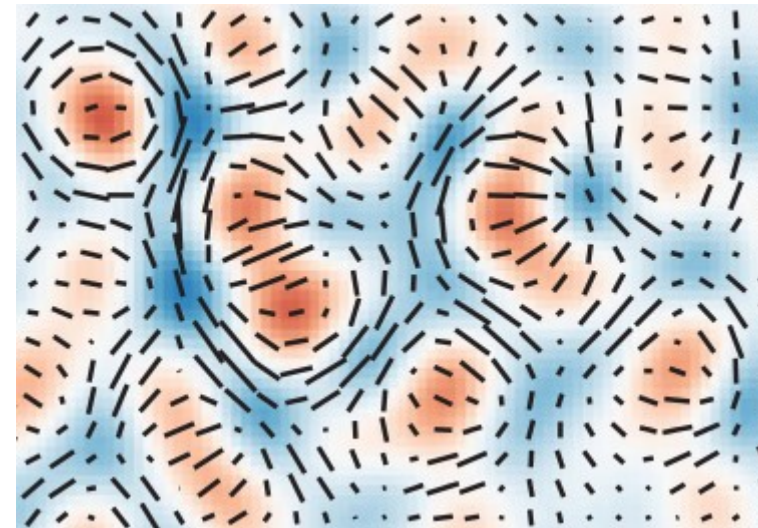
- Q, U polarization pattern can be decomposed in two “modes” with different symmetry properties
 - \mathbf{E} is generated by a polarization with vector properties (as the Electric field)
 - \mathbf{B} is generated by a polarization with pseudo-vector properties (as the Magnetic field)
 - Sign flip under a reflection ($\mathbf{x} \rightarrow -\mathbf{x}$)



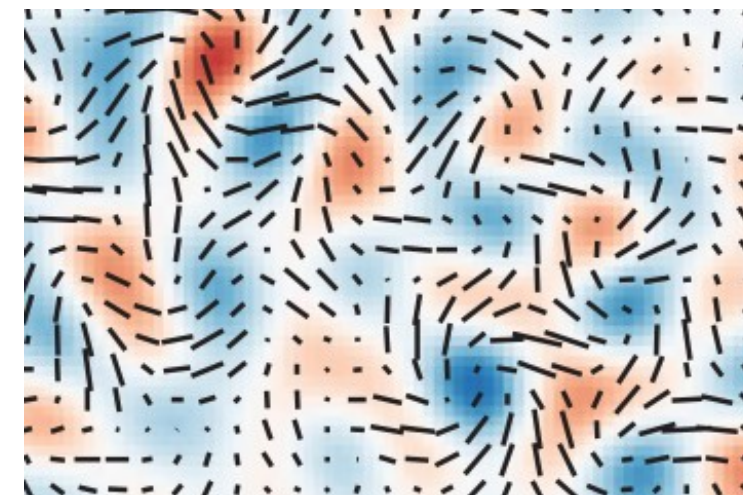
Polarization – E and B modes



planck



E-modes

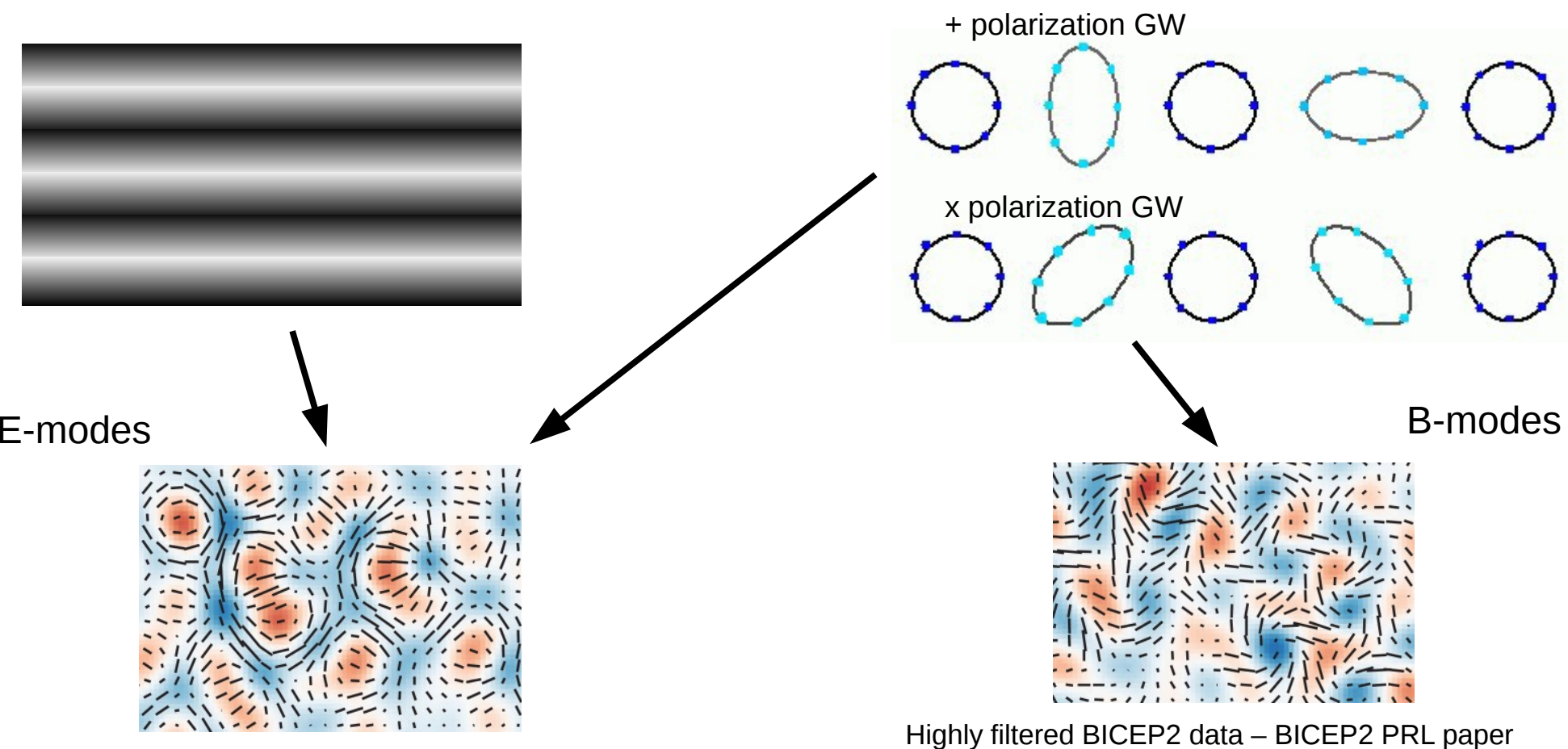


B-modes

Highly filtered BICEP2 data – BICEP2 PRL paper

Polarization – E and B modes

- Density (**scalar**) fluctuations, in linear regime, can't produce vorticity
- Gravitational Waves (**tensorial fluctuations**) produce vorticity, due their polarization



Challenge

- B-modes is the current challenge of the CMB experiment

- CMB radiation = 2.726 K
- CMB dipole = 3.346 mK (10^{-3})
- CMB anisotropy (rms) $\simeq 80 \mu\text{K}$ (10^{-5})
- CMB polarization E-modes (rms) $\simeq 1 \mu\text{K}$ (10^{-6})
- CMB polarization B-modes (rms) $< 0.2 \mu\text{K}$ (10^{-7})

Tensor to scalar ratio $r = T/S$

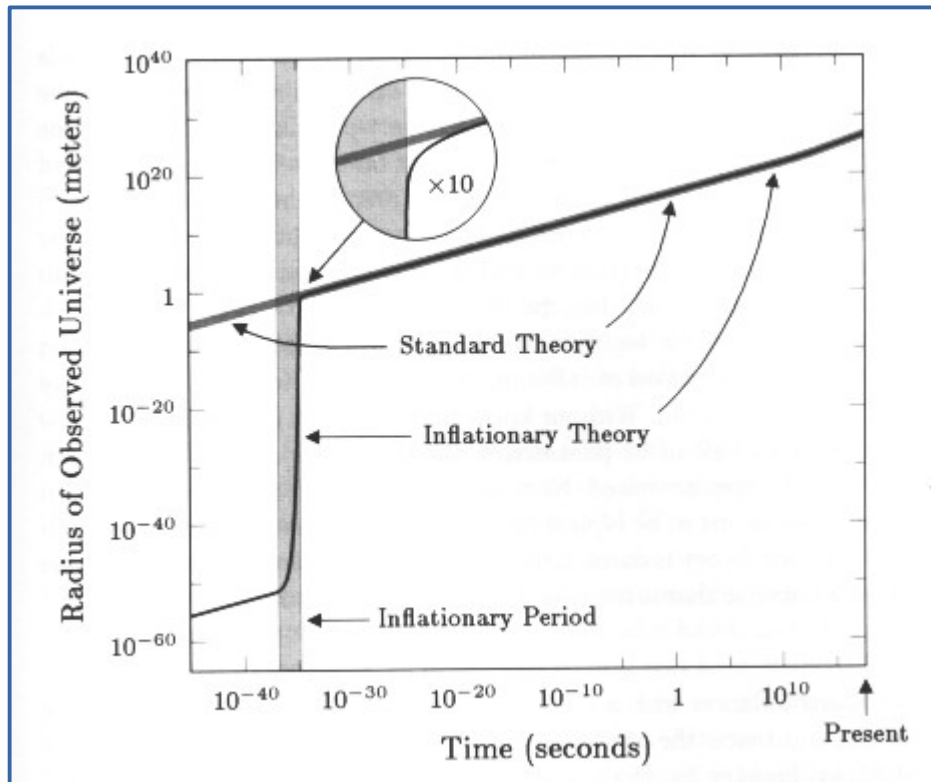
$$dl^2 = a^2(t)[1 + 2\zeta(x, t) + \dots][\delta_{ij} + h_{ij}(x, t) + \dots]dx^i dx^j$$

- $r = T/S = [\text{power in gravitational waves}]/[\text{power in curvature perturbation}]$

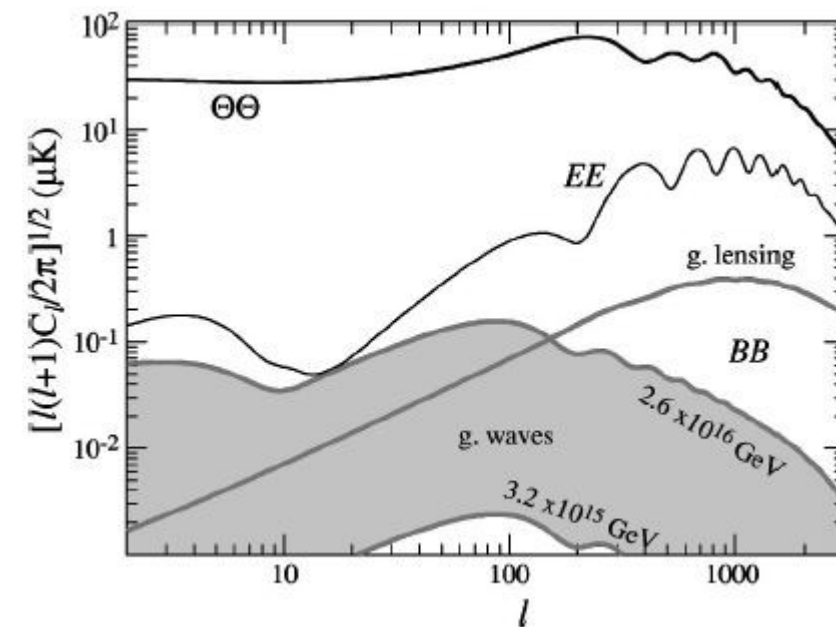
$$r = \frac{\langle h_{ij, k_0} h^{ij, k_0*} \rangle}{\langle |\zeta_{k_0}|^2 \rangle} \quad \text{with } k_0 = 0.002 \text{ Mpc}^{-1}$$

B-modes and inflation

- The presence of gravitational waves in the early universe is a prediction of the inflation
 - The **CMB polarization is an antenna for gravitational waves** in the early universe
 - The amplitude of primordial gravitational waves is encoded in the tensor/scalar parameter, r
 - Measuring **B -mode polarization** can shed light on the **inflation physics**



A. Guth



$$\left[\ell(\ell + 1)C_{\ell_{\text{peak}}}^{BB} \right]^{1/2} = 0.024(E_{\text{inf}}/10^{16} \text{ GeV})^2 \mu\text{K}$$

W. Hu et al. 2003

Constraints on inflation

- Planck 2013 results. XXII. Constraints on inflation, Accepted by A&A

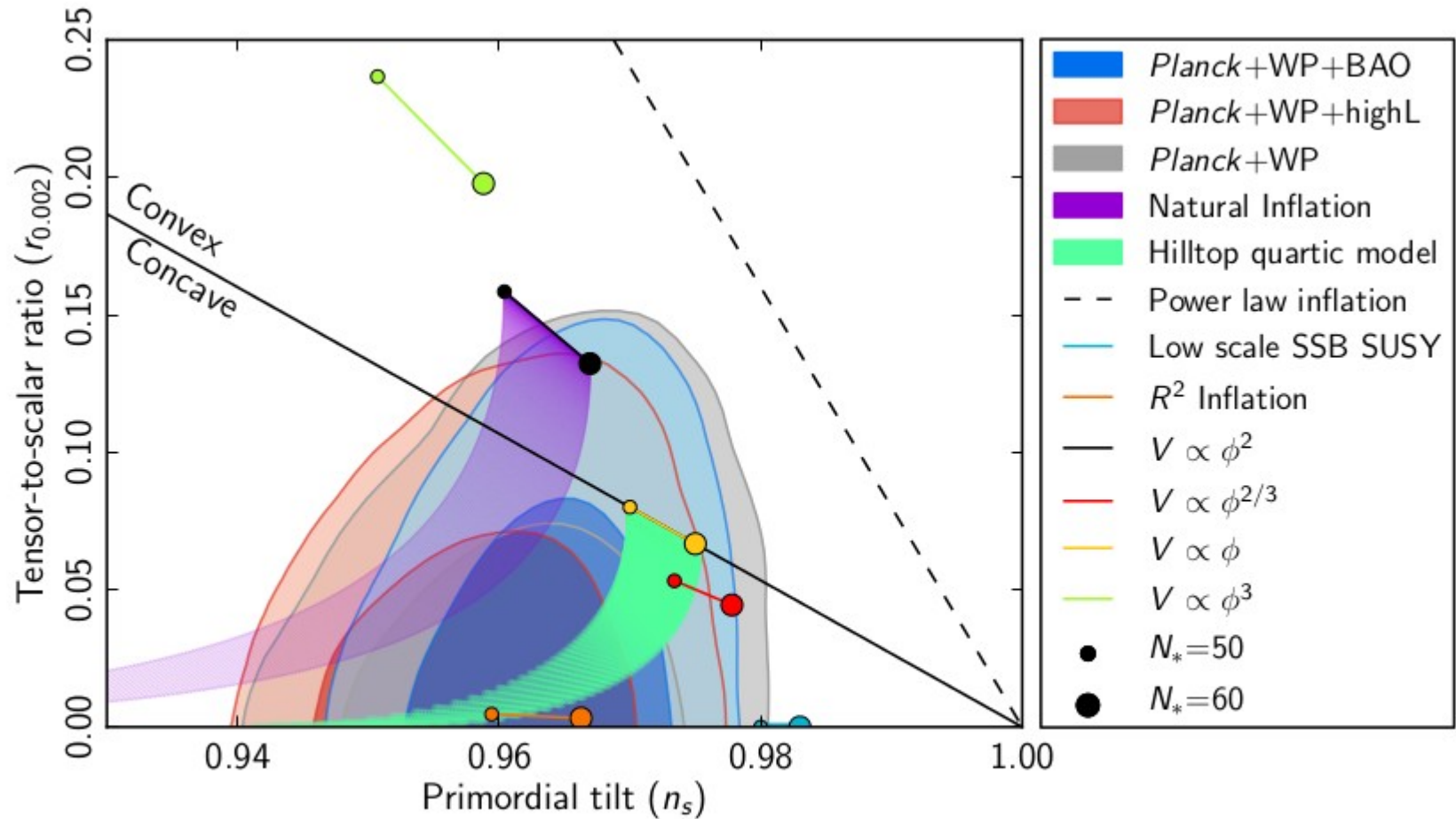


Fig. 1. Marginalized joint 68% and 95% CL regions for n_s and $r_{0.002}$ from *Planck* in combination with other data sets compared to the theoretical predictions of selected inflationary models.

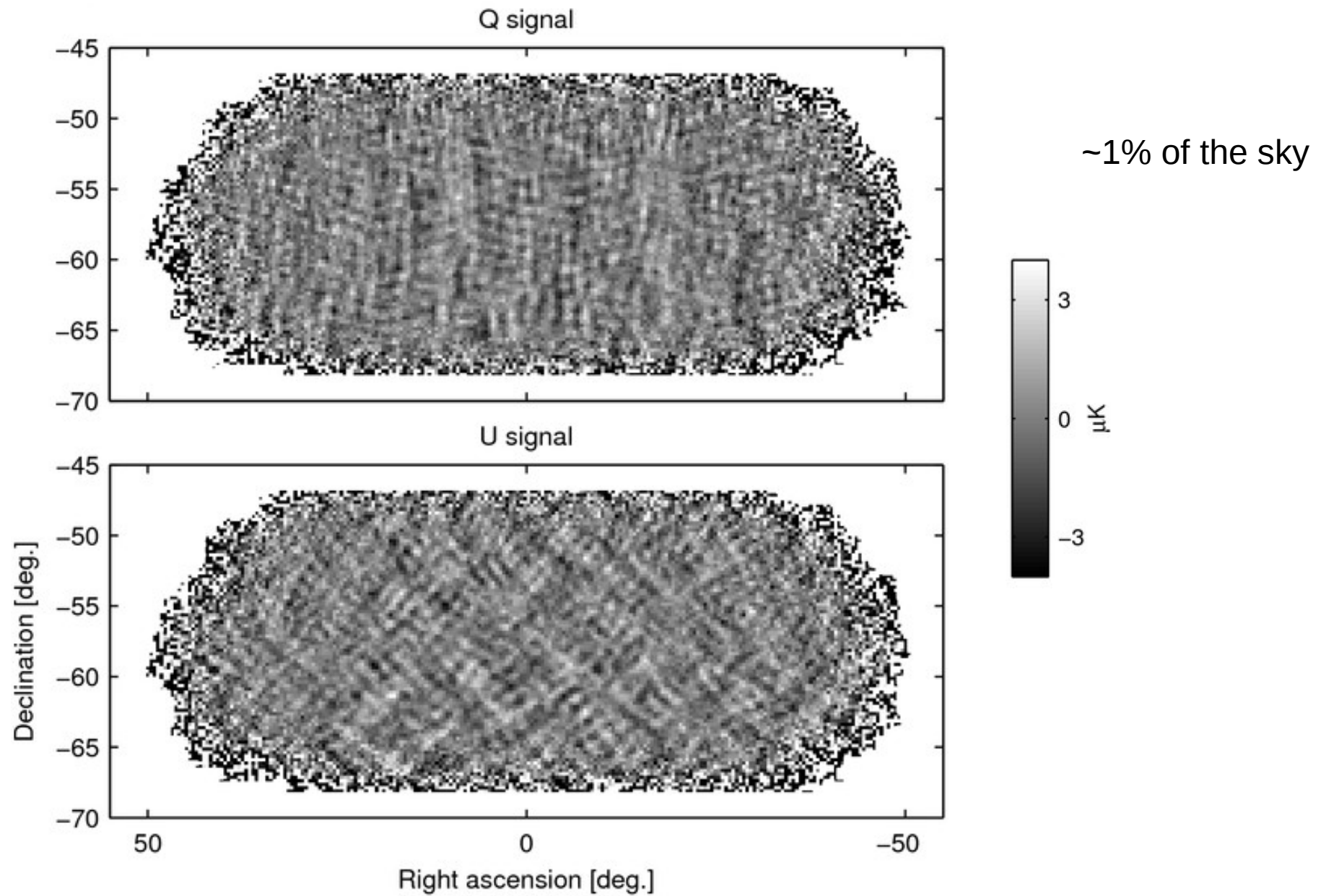


BICEP2 results

BICEP2 Stokes parameters maps



planck

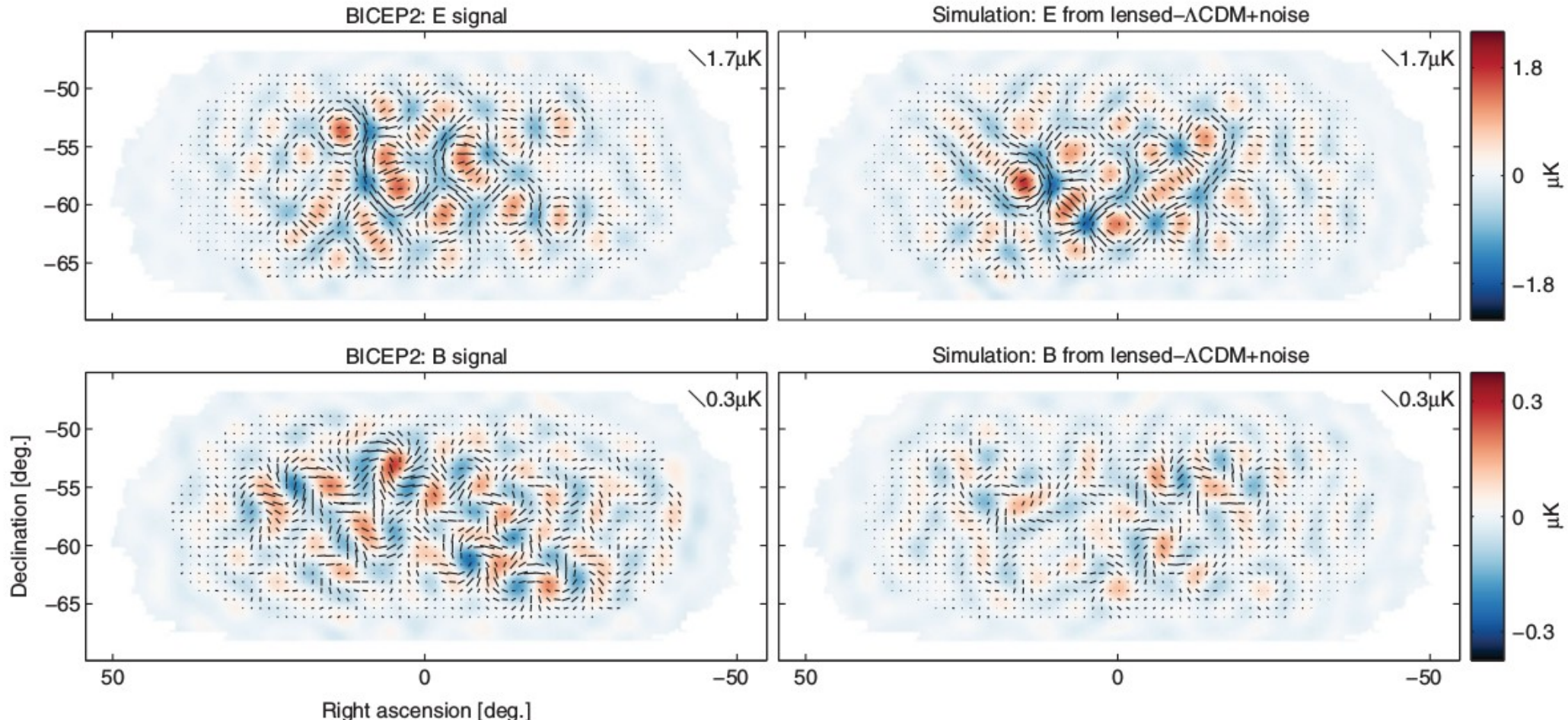


BICEP2 E/B modes maps


planck

PRL 112, 241101 (2014)

PHYSICAL REVIEW LETTERS

week ending
20 JUNE 2014

BICEP2 B-modes angular power

- B-modes are in fact made of two components
 - Primordial gravitational waves
 - Measured by BICEP2
 - Lensing effects on “standard” E-mode polarization
 - Recently observed by other ground based telescopes

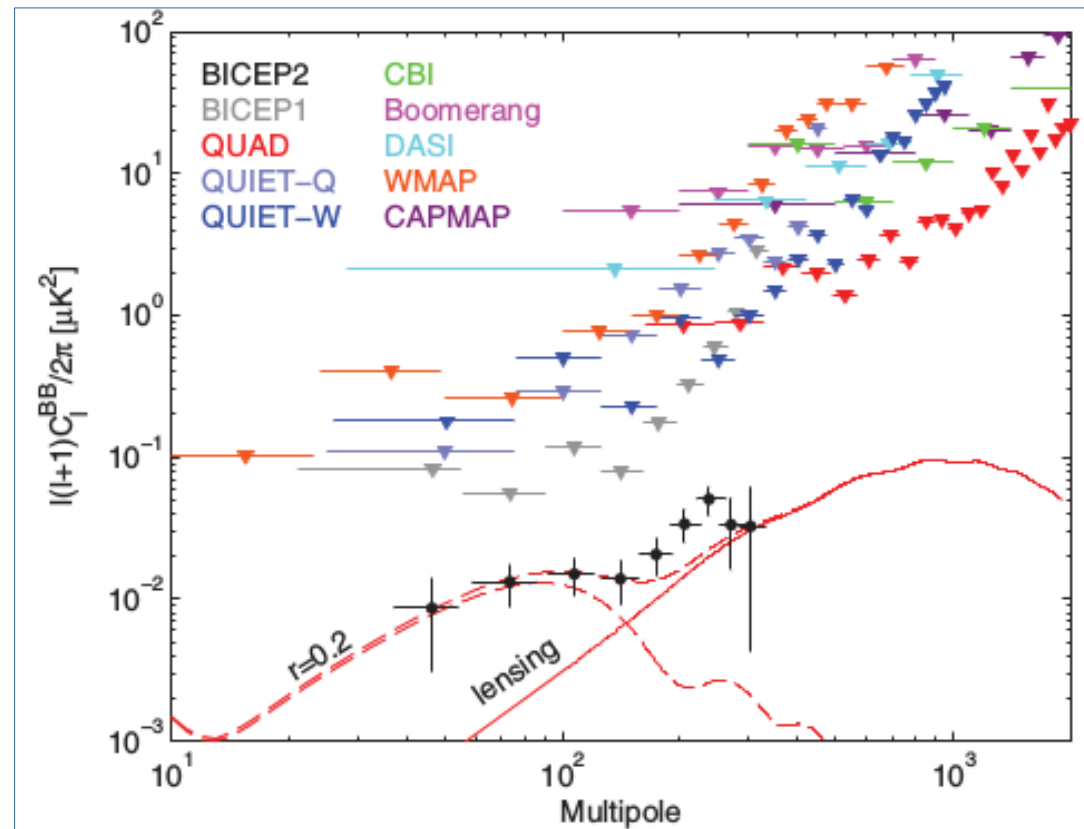


FIG. 14 (color). BICEP2 BB auto spectra and 95% upper limits from several previous experiments [2,40,42,43,47,49–51,107]. The curves show the theory expectations for $r = 0.2$ and lensed ΛCDM . The BICEP2 uncertainties include sample variance on an $r = 0.2$ contribution.

BICEP2 r significance

PRL 112, 241101 (2014)

PHYSICAL REVIEW LETTERS

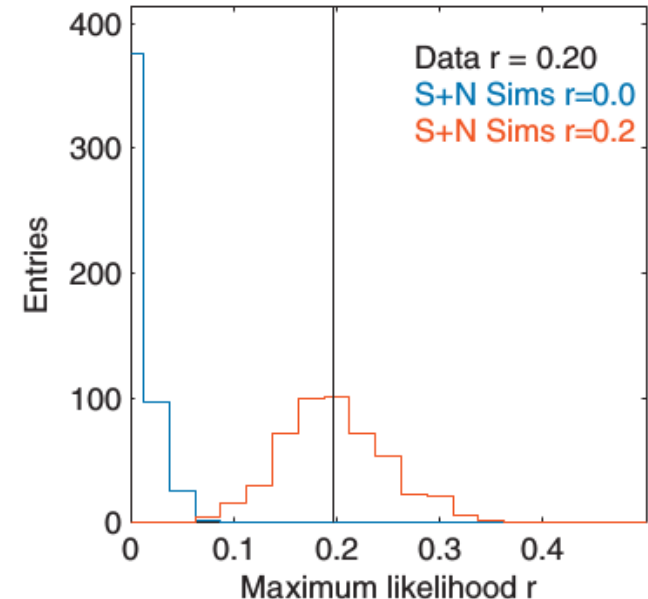
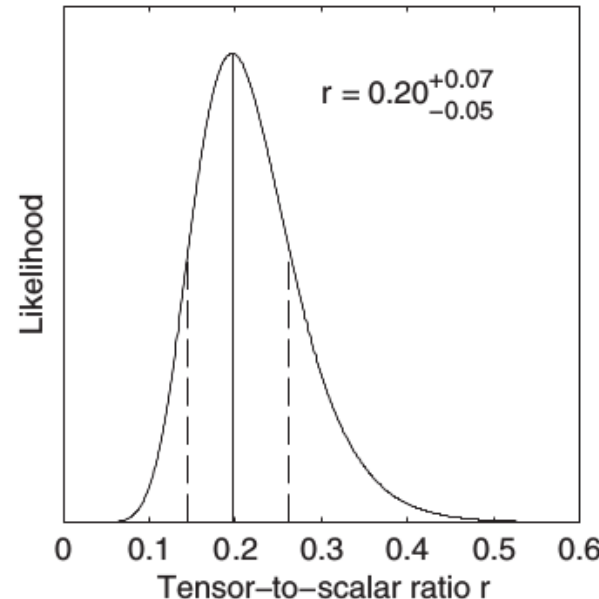
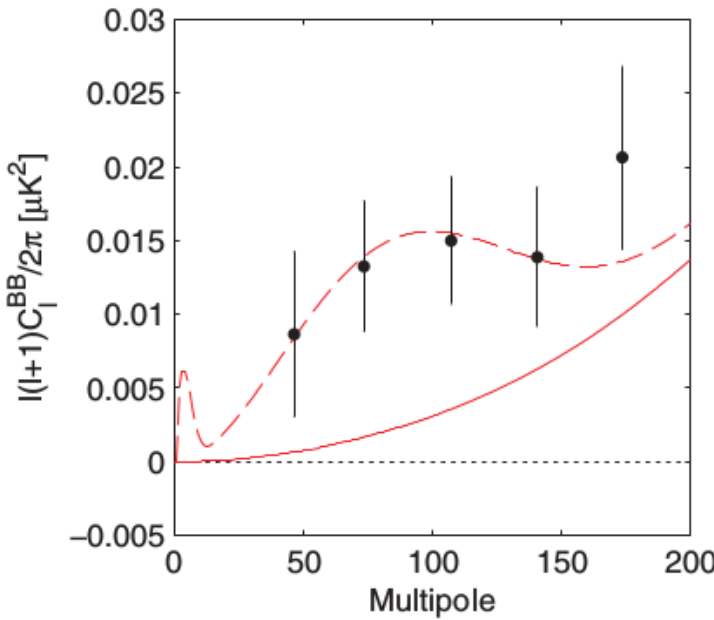
week ending
20 JUNE 2014

FIG. 10 (color). Left: The BICEP2 band powers plotted with the maximum likelihood lensed- Λ CDM + $r = 0.20$ model. The uncertainties are taken from that model and hence include sample variance on the r contribution. Middle: The constraint on the tensor-to-scalar ratio r . The maximum likelihood and $\pm 1\sigma$ interval is $r = 0.20^{+0.07}_{-0.05}$, as indicated by the vertical lines. Right: Histograms of the maximum likelihood values of r derived from lensed- Λ CDM + noise simulations with $r = 0$ (blue) and adding $r = 0.2$ (red). The maximum likelihood value of r for the real data is shown by the vertical line.

BICEP2 results, June 2014

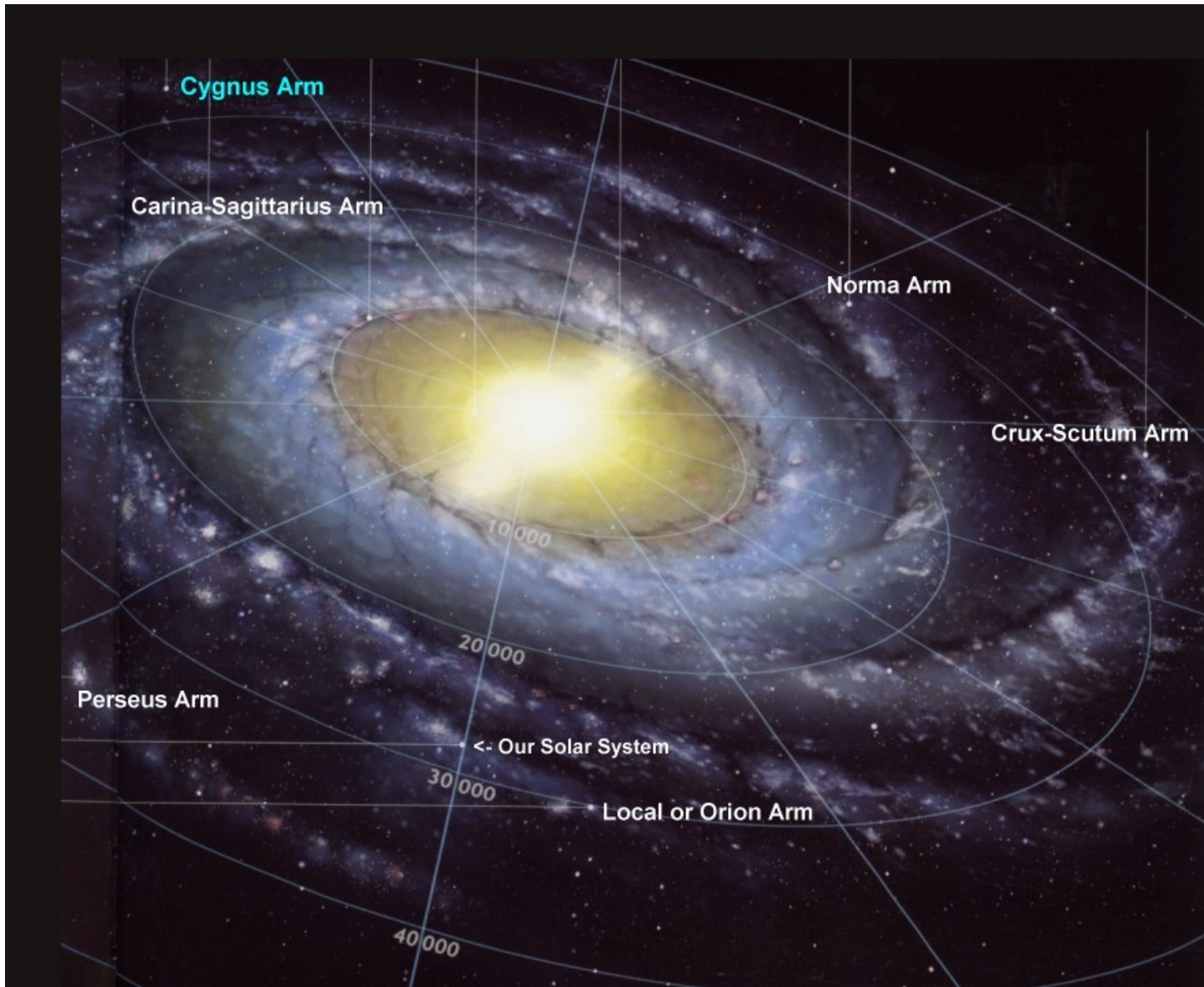


- Accounting for the contribution of foreground dust will shift this value downward by an amount which will be better constrained with upcoming data sets.
- If the origin is in tensors, as favored by the evidence presented above, it heralds a new era of B-mode cosmology. However, if these B modes represent evidence of a high-dust foreground, it reveals the scale of the challenges that lie ahead.

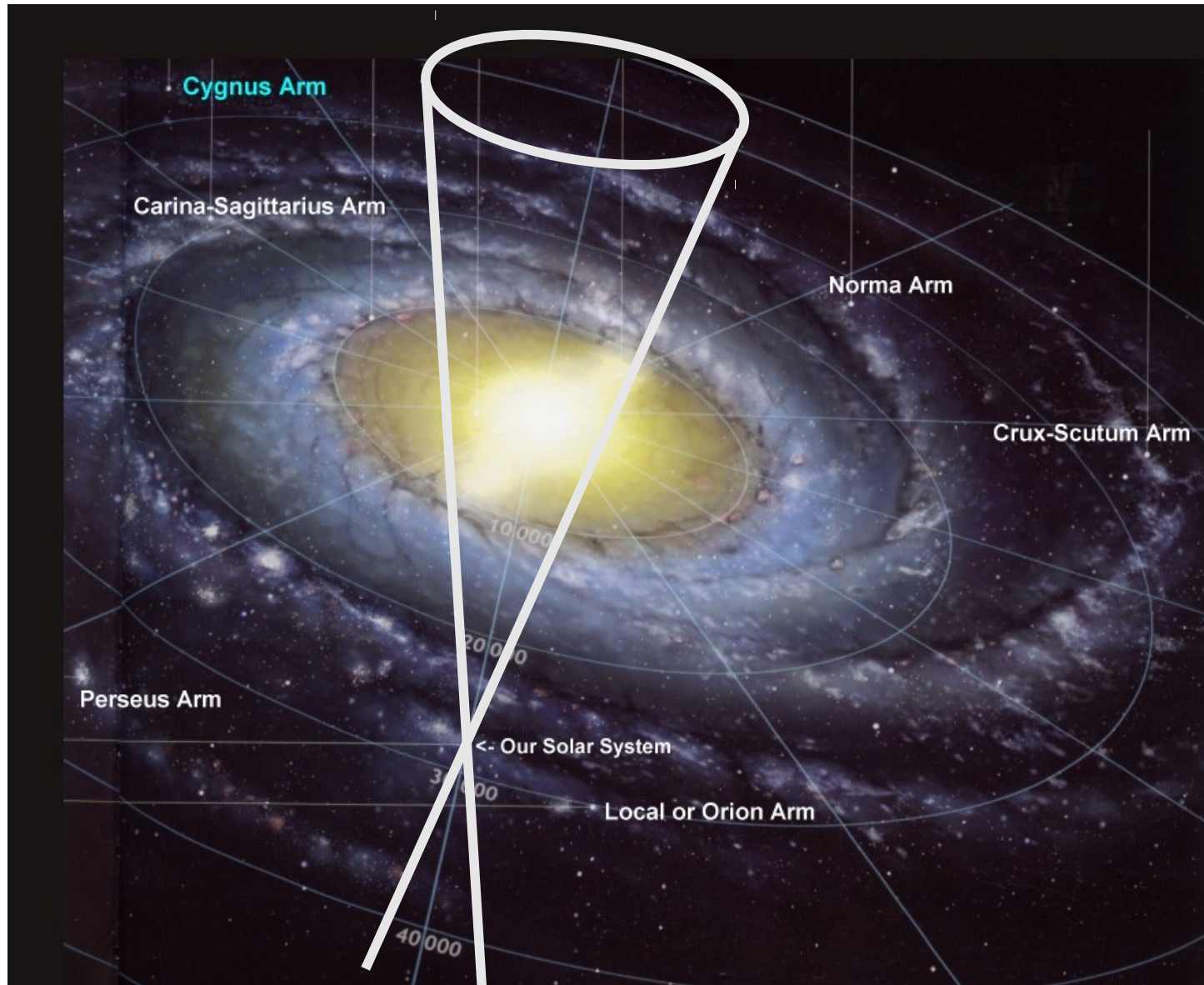


Interstellar dust polarization measurement with Planck

Observing through the Milky Way



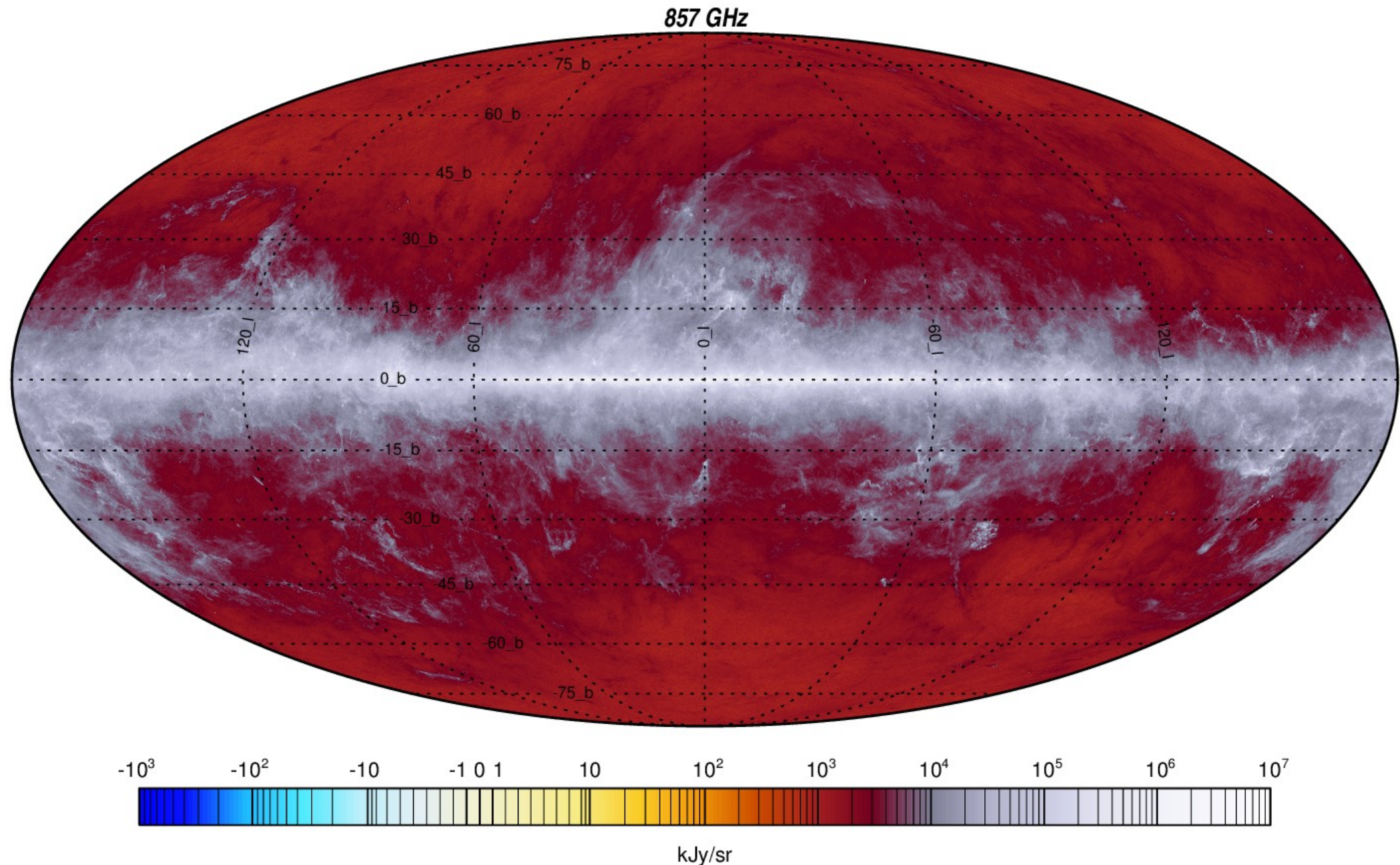
Observing through the Milky Way



Galactic thermal dust emission



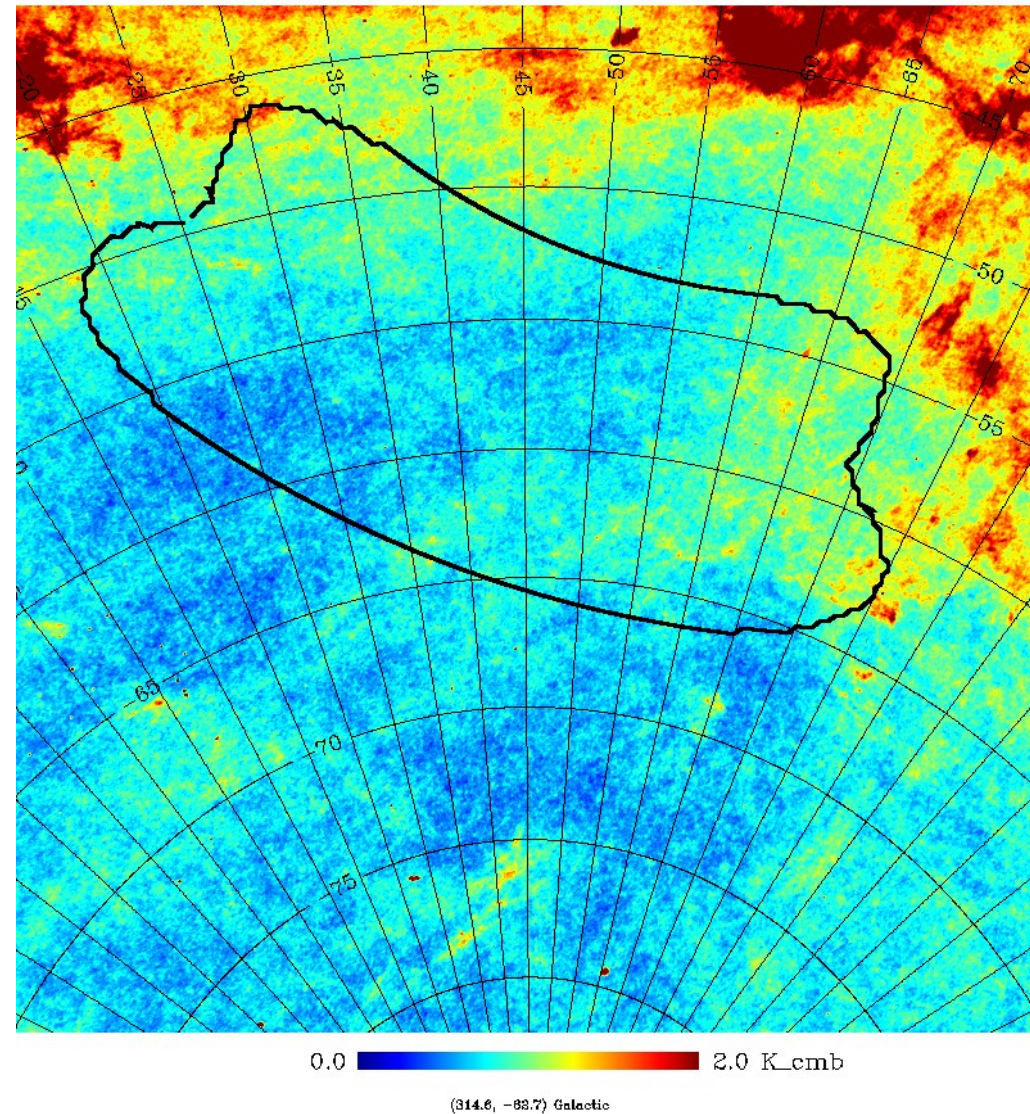
planck



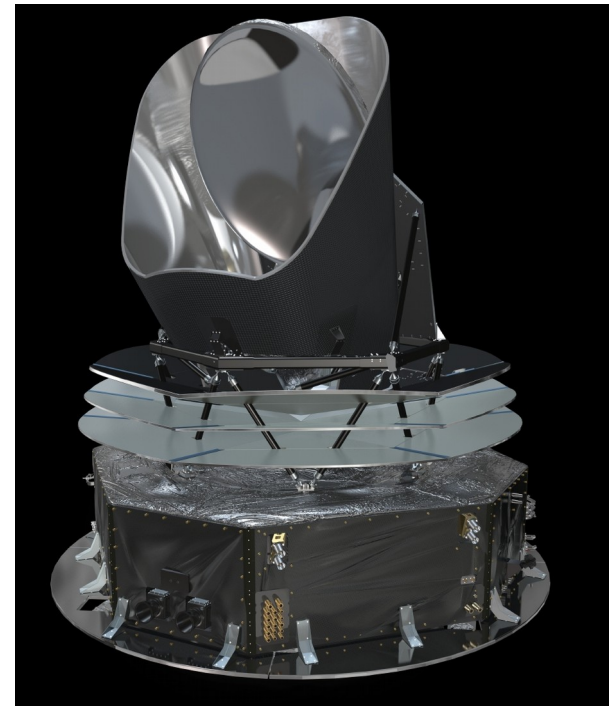
Galactic thermal dust emission



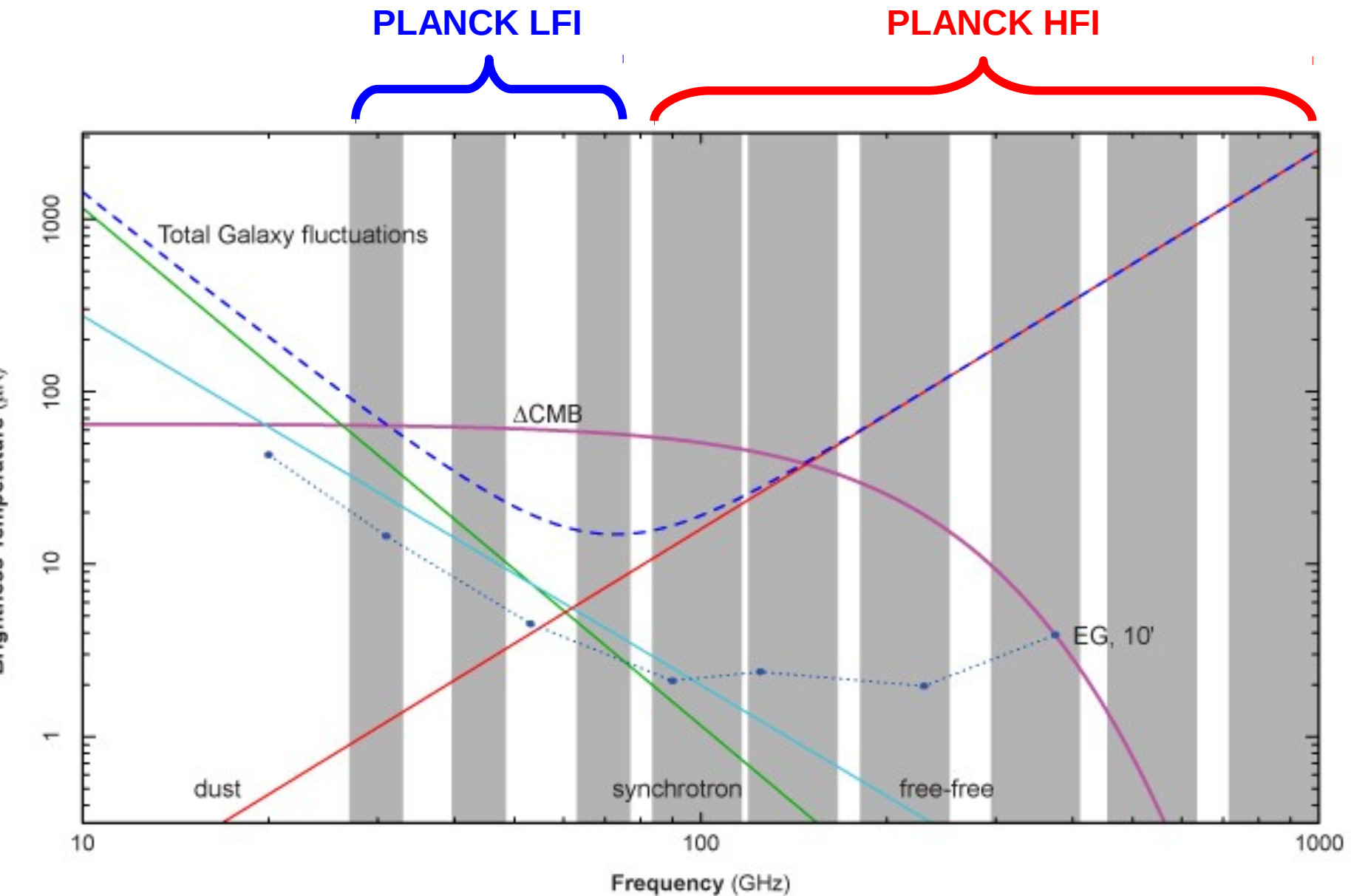
Planck 857 GHz – BICEP2 region – Galactic coordinates



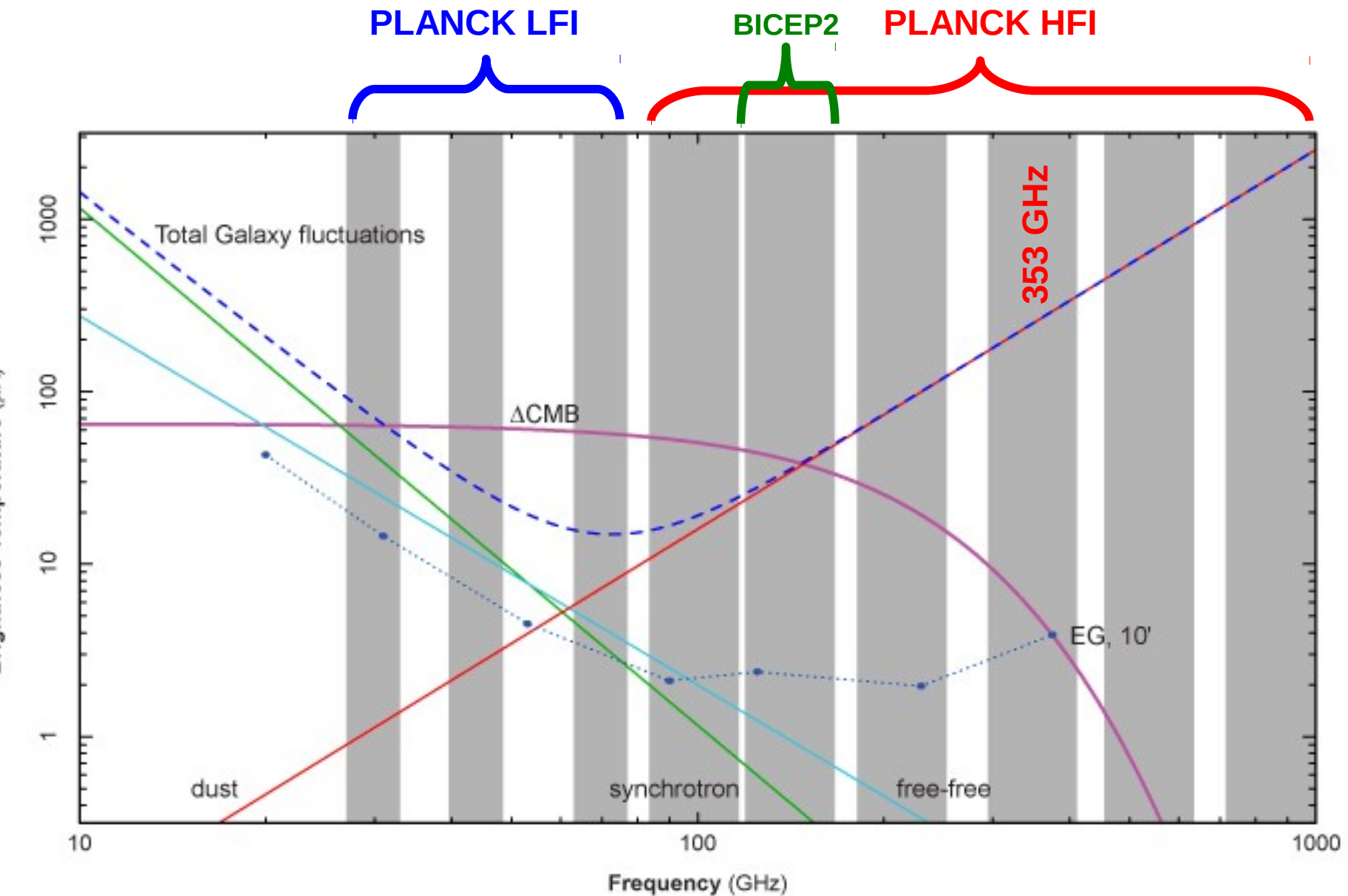
- European Space Agency **satellite** for microwave observation
 - (30 to 1000 GHz)
- Planck observed the full sky in the microwaves, with 9 bands in intensity and 7 bands in polarization
- The main goal is the measurement of the **CMB anisotropy and polarization**
- Planck has a polarized channel at 353 GHz very useful to measure **dust polarization**
- Operations: 2009-2013
- Data delivery
 - 2013, nominal mission, no polarization
 - Dec 2014, full mission, with polarization



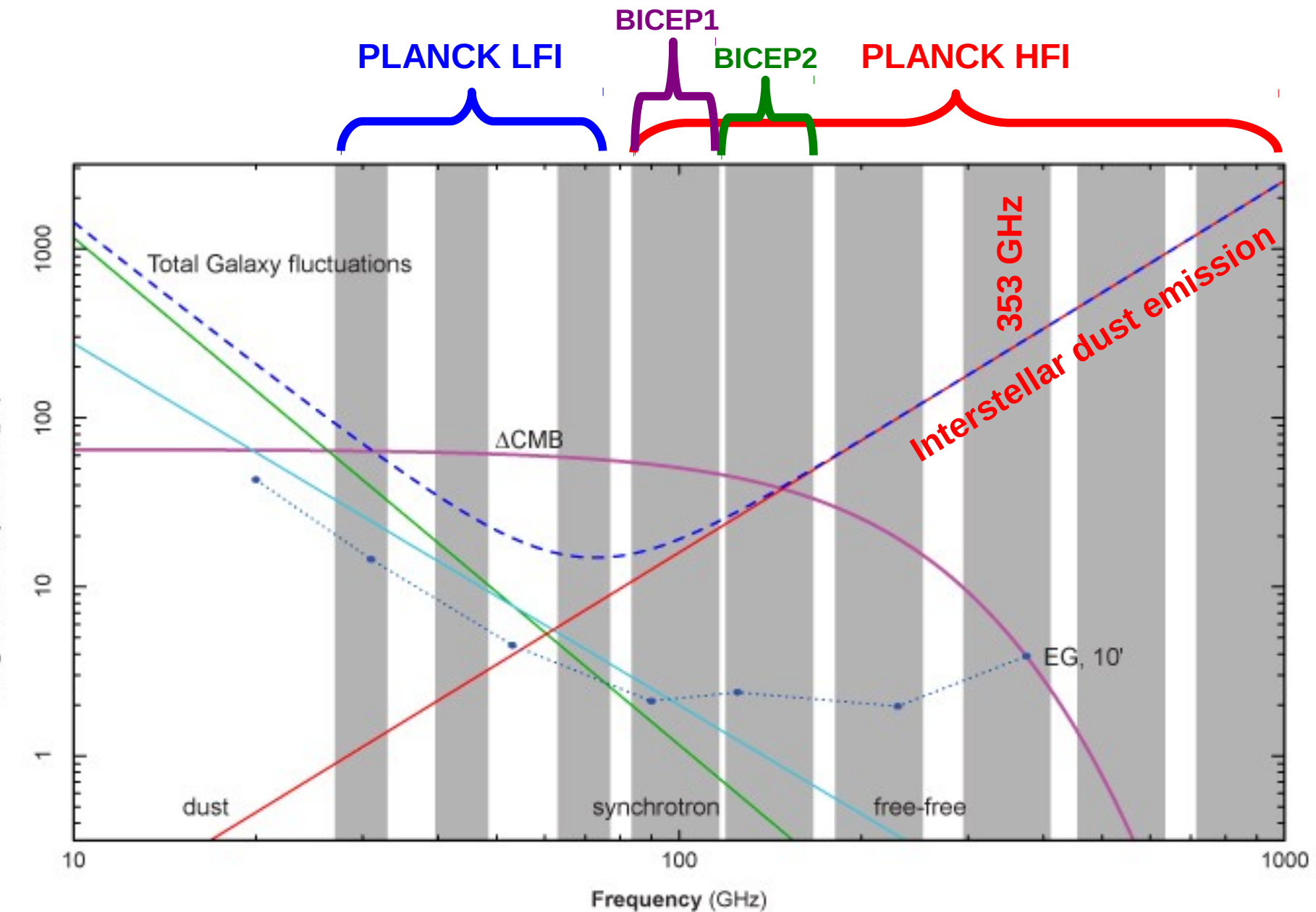
Observation bands



Observation bands



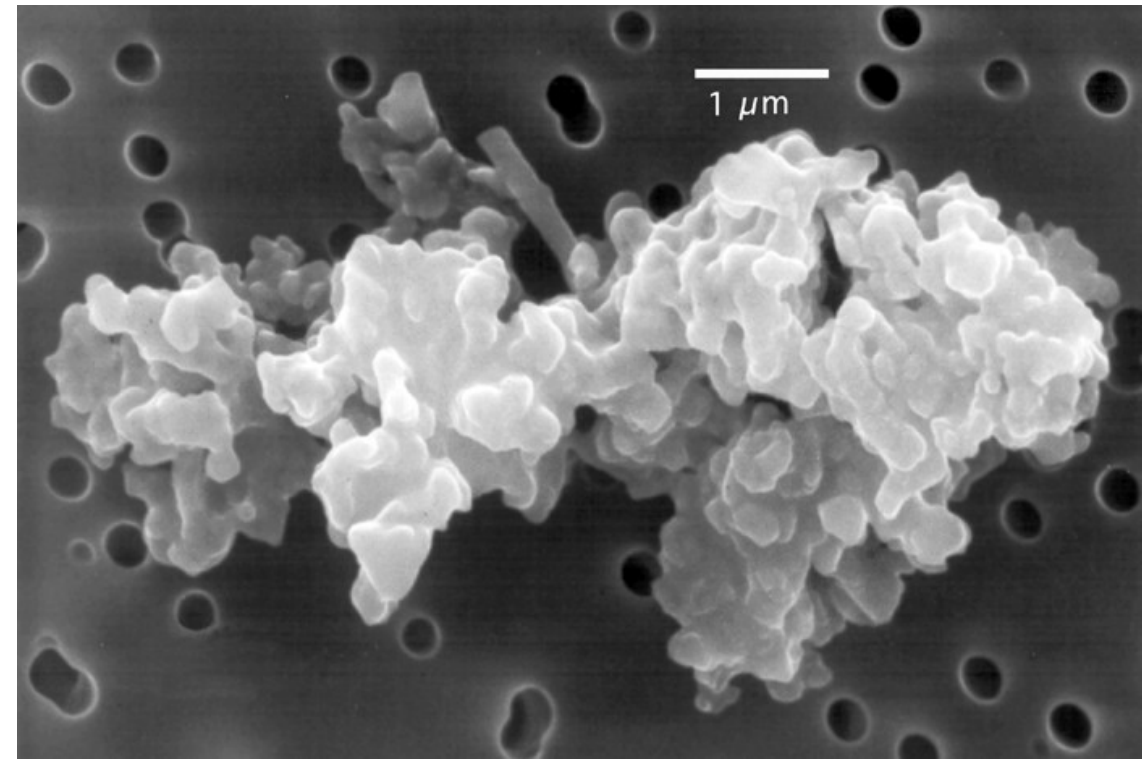
Observation bands



Interstellar dust

- Interstellar medium in the Milky Way
 - 500 000 hydrogen atoms/m³ (gas)
 - 100 dust grains/km³
 - (solid macroscopic particles composed of dielectric and refractory materials)
 - Dust grains are a significant fraction of the interstellar medium, 1% by mass

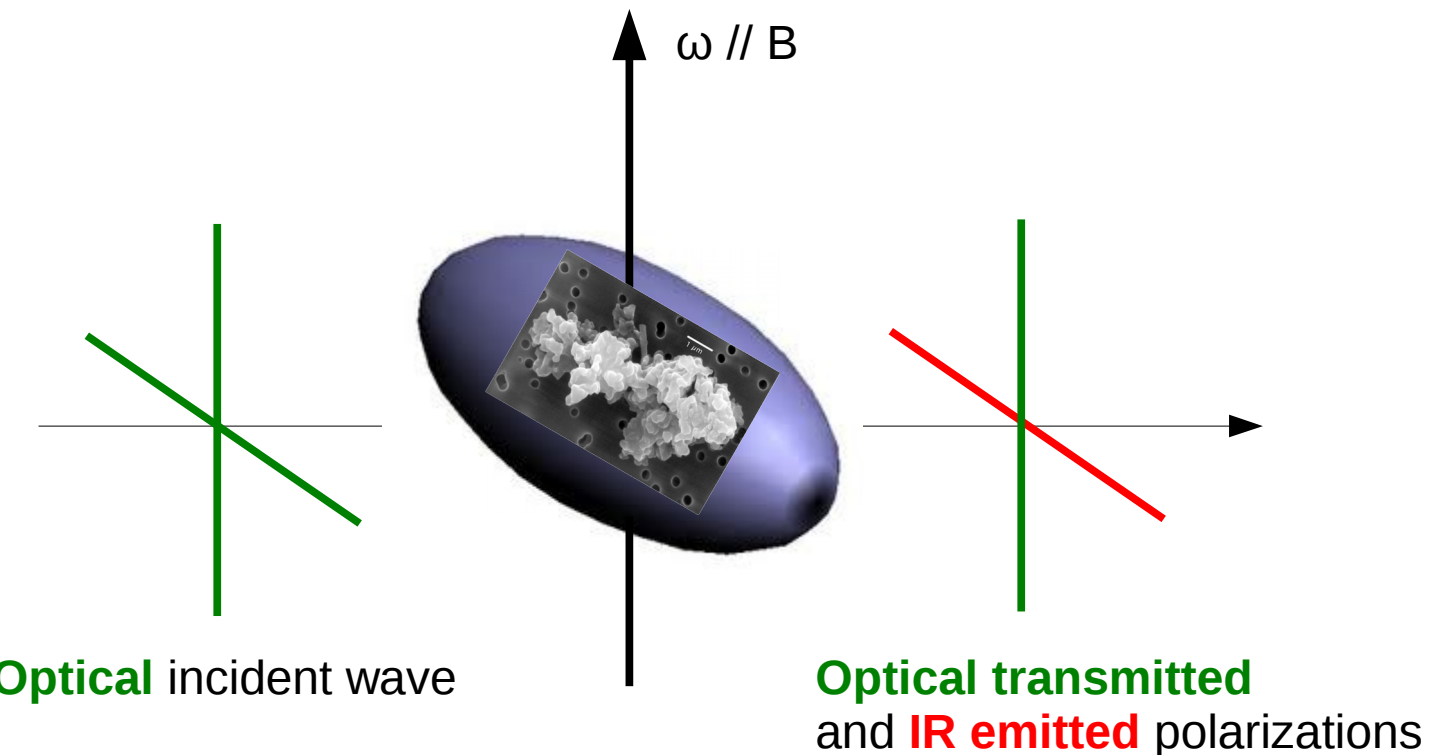
- Interstellar dust grains are believed to originate from
 - stellar winds of plasma flowing out from stars, planetary nebulae, novae and supernovae.
 - These plasmas contain some heavy elements which then condense to grains of iron and silicates.



Porous chondrite interplanetary dust particle
 Donald E. Brownlee, University of Washington, Seattle, and
 Elmar Jessberger, Institut für Planetologie, Münster, Germany

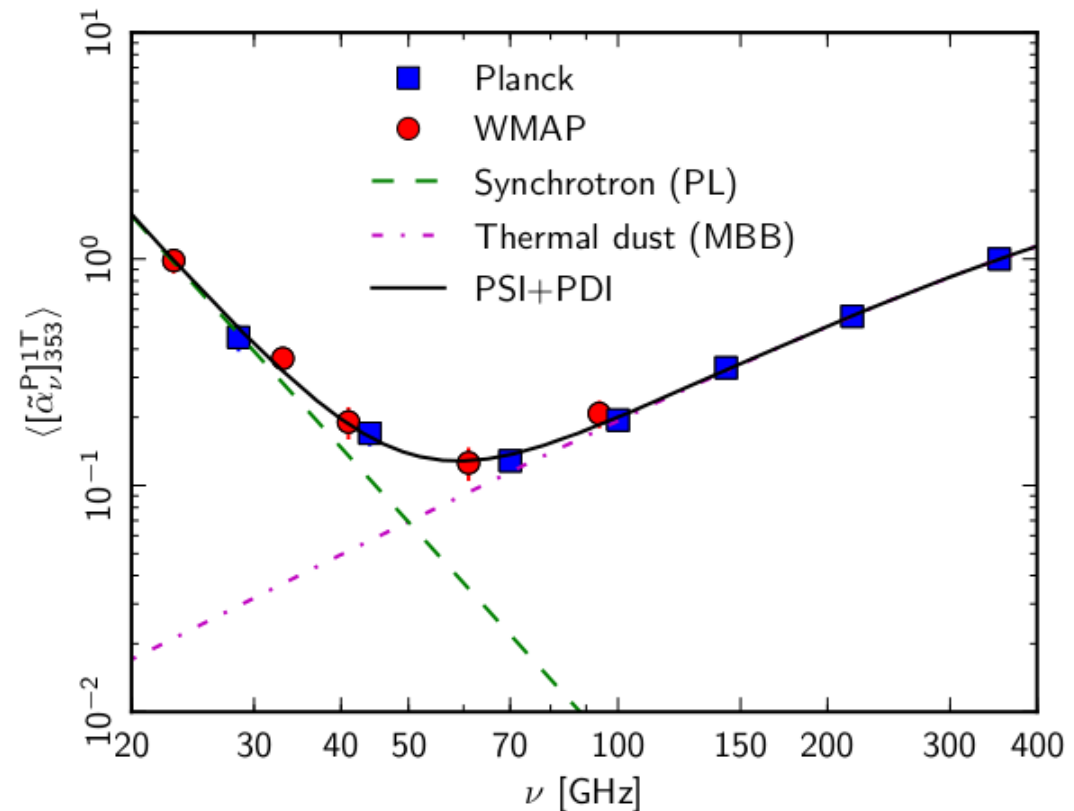
Interstellar dust polarization

- The interstellar dust grains spins with short axis aligned with the magnetic field
 - Absorption and emission are larger along the long axis
 - Optical light transmitted is polarized parallel to magnetic field
 - IR light emitted is polarized orthogonal to magnetic field



Frequency spectrum in polarization

- The best Planck Dust observations are made at 353 GHz
- To extrapolate the contamination at lower frequency, the spectral trend must be properly estimated
 - <http://arxiv.org/abs/1405.0874>: Planck collaboration, Frequency dependence of thermal emission from Galactic dust in intensity and polarization (May 5, 2014), submitted to A&A



Frequency spectrum in polarization

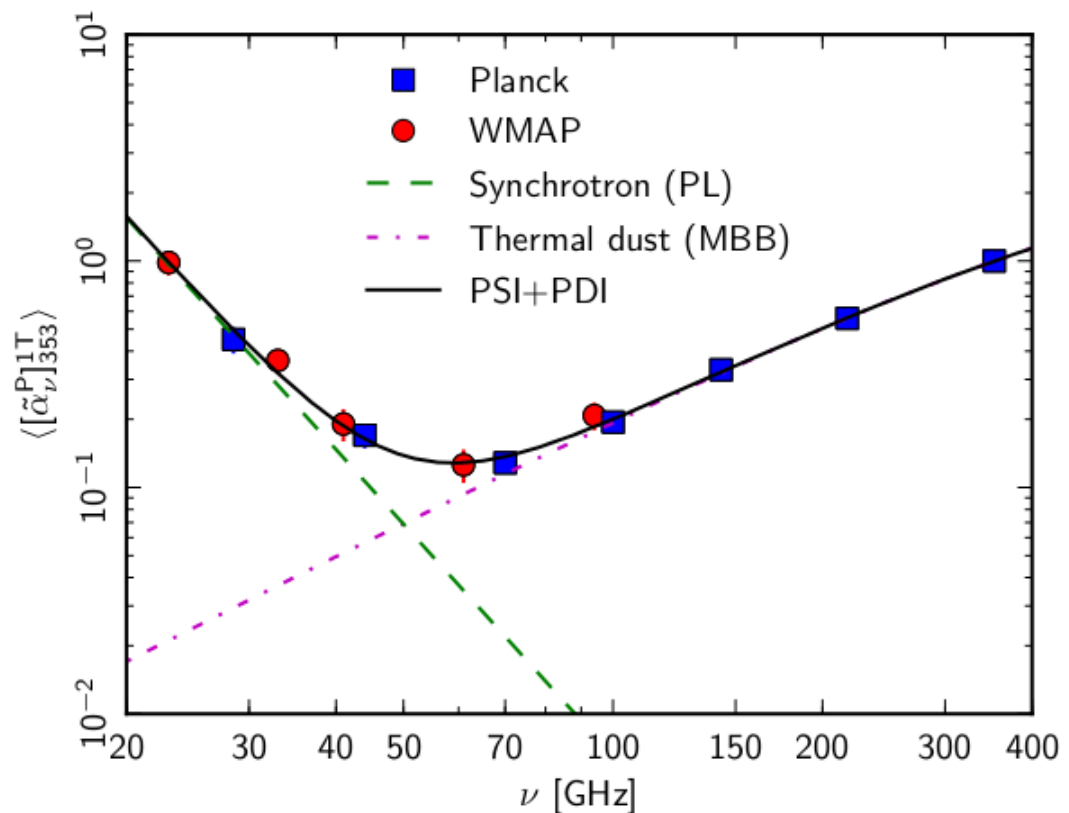
- Based on a **Cross Correlation technique**, correlating each map with Intensity and Polarization maps (Stokes Q, U) measured at 353 GHz, and assuming that dust has a Modified Black Body spectrum:

$$[Q_d, U_d] \propto \nu^{\beta_d} B_\nu(T_d)$$

$$T_d = 19.6 \text{ K}$$

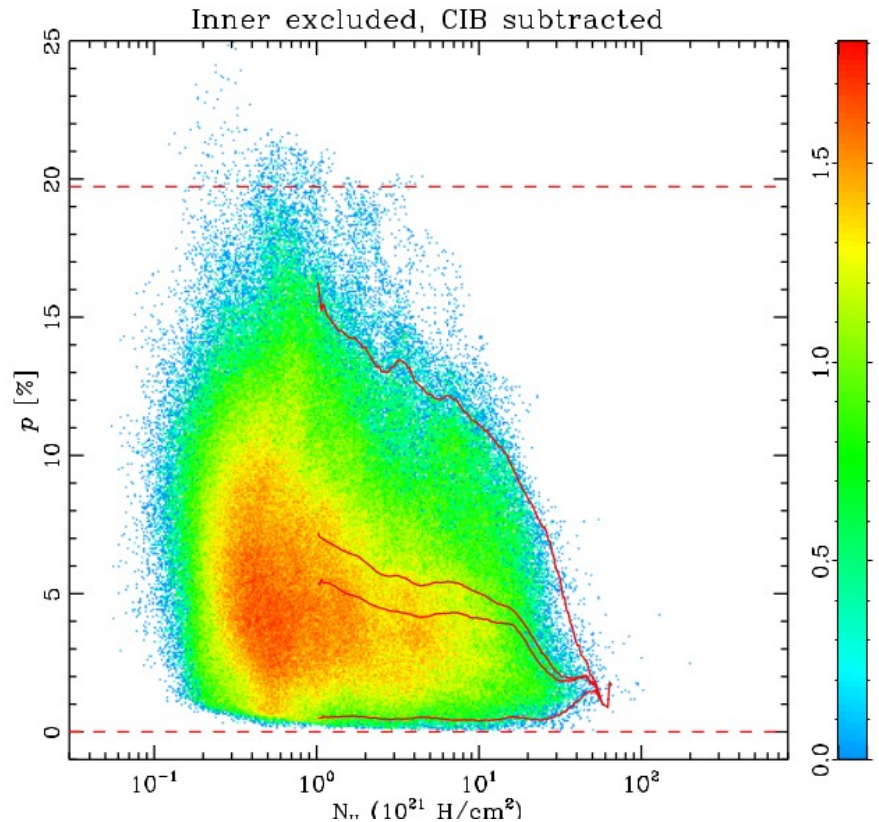
This is a parameter, not a physical temperature (although very similar)

$$\beta_d = 1.59 \pm 0.17$$



Planck interstellar dust polarization

- <http://arxiv.org/abs/1405.0871>
- Planck intermediate results. XIX. An overview of the polarized thermal emission from Galactic dust
- Submitted to A&A in May 2014

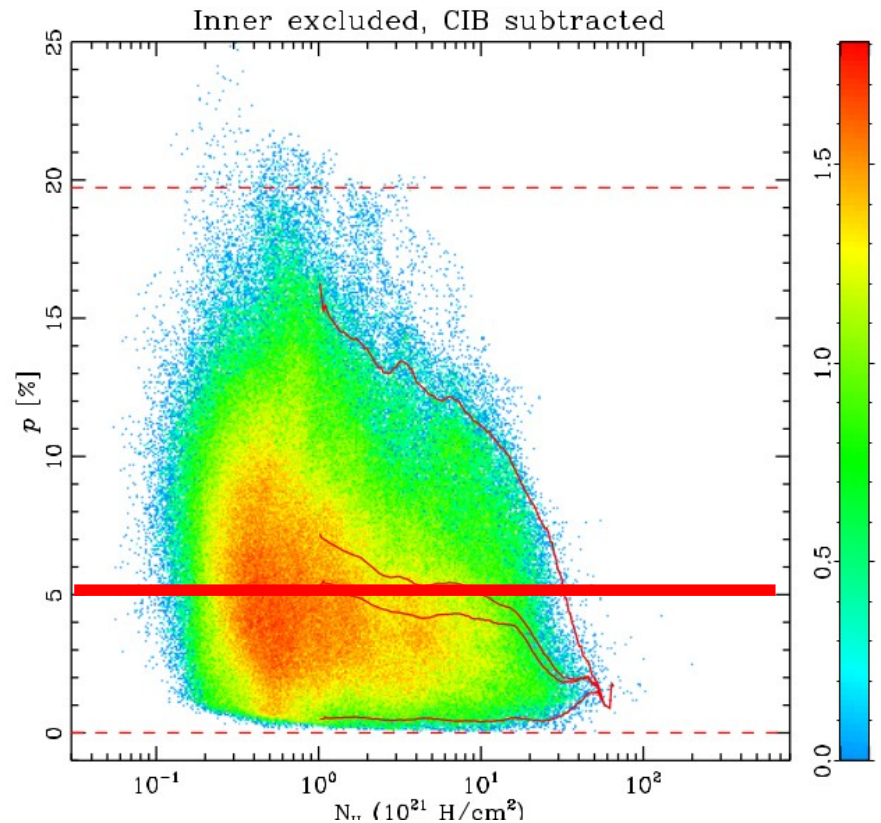


- Polarization fraction is higher in thinner column density regions

Planck interstellar dust polarization

- <http://arxiv.org/abs/1405.0871>
- Planck intermediate results. XIX. An overview of the polarized thermal emission from Galactic dust
- Submitted to A&A in May 2014

**BICEP2 models
polarization fraction**



- Polarization fraction is higher in thinner column density regions

Recent Planck results

8v1 [astro-ph.CO] 19 Sep 2014

Planck intermediate results. XXX.

The angular power spectrum of polarized dust emission at intermediate and high Galactic latitudes

Planck Collaboration: R. Adam⁷⁶, P. A. R. Ade⁸⁶, N. Aghanim⁶¹, M. Arnaud⁷⁴, J. Aumont⁶¹*, C. Baccigalupi⁸⁵, A. J. Banday^{94,9}, R. B. Barreiro⁶⁷, J. G. Bartlett^{1,68}, N. Bartolo³¹, E. Battaner^{97,98}, K. Benabed^{62,93}, A. Benoit-Lévy^{23,62,93}, J.-P. Bernard^{94,9}, M. Bersanelli^{34,51}, P. Bielewicz^{94,9,85}, A. Bonaldi⁶⁹, L. Bonavera⁶⁷, J. R. Bond⁸, J. Borrill^{14,89}, F. R. Bouchet^{62,93}, F. Boulanger⁶¹, A. Bracco⁶¹, M. Bucher¹, C. Burigana^{50,32,52}, R. C. Butler⁵⁰, E. Calabrese⁹¹, J.-F. Cardoso^{75,1,62}, A. Catalano^{76,73}, A. Challinor^{64,70,12}, A. Chamballu^{74,16,61}, R.-R. Chary⁵⁹, H. C. Chiang^{26,6}, P. R. Christensen^{82,38}, D. L. Clements⁵⁸, S. Colombi^{62,93}, L. P. L. Colombo^{22,68}, C. Combet⁷⁶, F. Couchot⁷¹, A. Coulais⁷³, A. Curto^{5,67}, F. Cuttaia⁵⁰, L. Danese⁸⁵, R. D. Davies⁶⁹, R. J. Davis⁶⁹, P. de Bernardis³³, G. de Zotti^{47,85}, J. Delabrouille¹, J.-M. Delouis^{62,93}, F.-X. Désert⁵⁶, C. Dickinson⁶⁹, J. M. Diego⁶⁷, K. Dolag^{96,79}, H. Dole^{61,60}, S. Donzelli⁵¹, O. Doré^{68,11}, M. Douspis⁶¹, A. Ducout^{62,58}, J. Dunkley⁹¹, X. Dupac⁴¹, G. Efstathiou⁶⁴, F. Elsner^{62,93}, T. A. Enßlin⁷⁹, H. K. Eriksen⁶⁵, E. Falgarone⁷³, F. Finelli^{50,52}, O. Forni^{94,9}, M. Frailis⁴⁹, A. A. Fraisse²⁶, E. Franceschi⁵⁰, A. Frejsel⁸², S. Galeotta⁴⁹, S. Galli⁶², K. Ganga¹, T. Ghosh⁶¹, M. Giard^{94,9}, Y. Giraud-Héraud¹, E. Gjerløw⁶⁵, J. González-Nuevo^{67,85}, K. M. Górski^{68,99}, S. Gratton^{70,64}, A. Gregorio^{35,49,55}, A. Gruppuso⁵⁰, V. Guillet⁶¹, F. K. Hansen⁶⁵, D. Hanson^{80,68,8}, D. L. Harrison^{64,70}, G. Helou¹¹, S. Henrot-Versillé⁷¹, C. Hernández-Monteagudo^{13,79}, D. Herranz⁶⁷, E. Hivon^{62,93}, W. A. Holmes⁶⁸, K. M. Huffenberger²⁴, G. Hurier⁶¹, A. H. Jaffe⁵⁸, T. R. Jaffe^{94,9}, J. Jewell⁶⁸, W. C. Jones²⁶, M. Juvela²⁵, E. Keihänen²⁵, R. Keskitalo¹⁴, T. S. Kisner⁷⁸, R. Kneissl^{40,7}, J. Knoche⁷⁹, L. Knox²⁸, N. Krachmalnicoff³⁴, M. Kunz^{18,61,2}, H. Kurki-Suonio^{25,46}, G. Lagache⁶¹, J.-M. Lamarre⁷³, A. Lasenby^{5,70}, M. Lattanzi³², C. R. Lawrence⁶⁸, J. P. Leahy⁶⁹, R. Leonardi⁴¹, J. Lesgourgues^{92,84,72}, F. Levrier⁷³, M. Liguori³¹, P. B. Lilje⁶⁵, M. Linden-Vørnle¹⁷, M. López-Caniego⁶⁷, P. M. Lubin²⁹, J. F. Macías-Pérez⁷⁶, B. Maffei⁶⁹, D. Maino^{34,51}, N. Mandolesi^{50,4,32}, A. Mangilli⁶², M. Maris⁴⁹, P. G. Martin⁸, E. Martínez-González⁶⁷, S. Masi³³, S. Matarrese³¹, P. Mazzotta³⁶, A. Melchiorri^{33,53}, L. Mendes⁴¹, A. Mennella^{34,51}, M. Migliaccio^{64,70}, S. Mitra^{57,68}, M.-A. Miville-Deschénes^{61,8}, A. Moneti⁶², L. Montier^{94,9}, G. Morgante⁵⁰, D. Mortlock⁵⁸, A. Moss⁸⁷, D. Munshi⁸⁶, J. A. Murphy⁸¹, P. Naselsky^{82,38}, F. Nati³³, P. Natoli^{32,3,50}, C. B. Netterfield¹⁹, H. U. Nørgaard-Nielsen¹⁷, F. Noviello⁶⁹, D. Novikov⁵⁸, I. Novikov⁸², L. Pagano^{33,53}, F. Pajot⁶¹, R. Paladini⁵⁹, D. Paoletti^{50,52}, B. Partridge⁴⁵, F. Pasian⁴⁹, G. Patanchon¹, T. J. Pearson^{11,59}, O. Perdereau⁷¹, L. Perotto⁷⁶, F. Perrotta⁸⁵, V. Pettorino⁴⁴, F. Piacentini³³, M. Piat¹, E. Pierpaoli²², D. Pietrobon⁶⁸, S. Plaszczynski⁷¹, E. Pointecouteau^{94,9}, G. Polenta^{3,48}, N. Ponthieu^{61,56}, L. Popa⁶³, G. W. Pratt⁷⁴, S. Prunet^{62,93}, J.-L. Puget⁶¹, J. P. Rachén^{20,79}, W. T. Reach⁹⁵, R. Rebolo^{66,15,39}, M. Remazeilles^{69,61,1}, C. Renault⁷⁶, A. Renzi^{37,54}, S. Ricciardi⁵⁰, I. Ristorcelli^{94,9}, G. Rocha^{68,11}, C. Rosset¹, M. Rossetti^{34,51}, G. Roudier^{1,73,68}, B. Rouillé d'Orfeuil⁷¹, J. A. Rubiño-Martín^{66,39}, B. Rusholme⁵⁹, M. Sandri⁵⁰, D. Santos⁷⁶, M. Savelainen^{25,46}, G. Savini⁸³, D. Scott²¹, J. D. Soler⁶¹, L. D. Spencer⁸⁶, V. Stolyarov^{5,70,90}, R. Stompor¹, R. Sudiwala⁸⁶, R. Sunyaev^{79,88}, D. Sutton^{64,70}, A.-S. Suur-Uski^{25,46}, J.-F. Sygnet⁶², J. A. Tauber⁴², L. Terenzi^{43,50}, M. Tomasi^{34,51}, M. Tristram⁷¹, M. Tucci^{18,71}, J. Tuovinen¹⁰, L. Valenziano⁵⁰, J. Valiviita^{25,46}, B. Van Tent⁷⁷, L. Vibert⁶¹, P. Vielva⁶⁷, F. Villa⁵⁰, L. A. Wade⁶⁸, B. D. Wandelt^{62,93,30}, R. Watson⁶⁹, I. K. Wehus⁶⁸, M. White²⁷, S. D. M. White⁷⁹, D. Yvon¹⁶, A. Zacchei⁴⁹, and A. Zonca²⁹

(Affiliations can be found after the references)

Preprint online version: 19 September 2014

Recent Planck results

- Statistical analysis of the Dust polarization, in clean regions, in terms of angular power spectra
 - General properties for large sky fractions
 - Analysis in small sky patches, in search for “clean” windows in faintest dust-emitting regions
 - Analysis of the level of dust polarization in the specific field recently targeted by the BICEP2 experiment

Planck masks selection

Carbon Monoxide regions removed

Point Sources removed

Different level of dust intensity

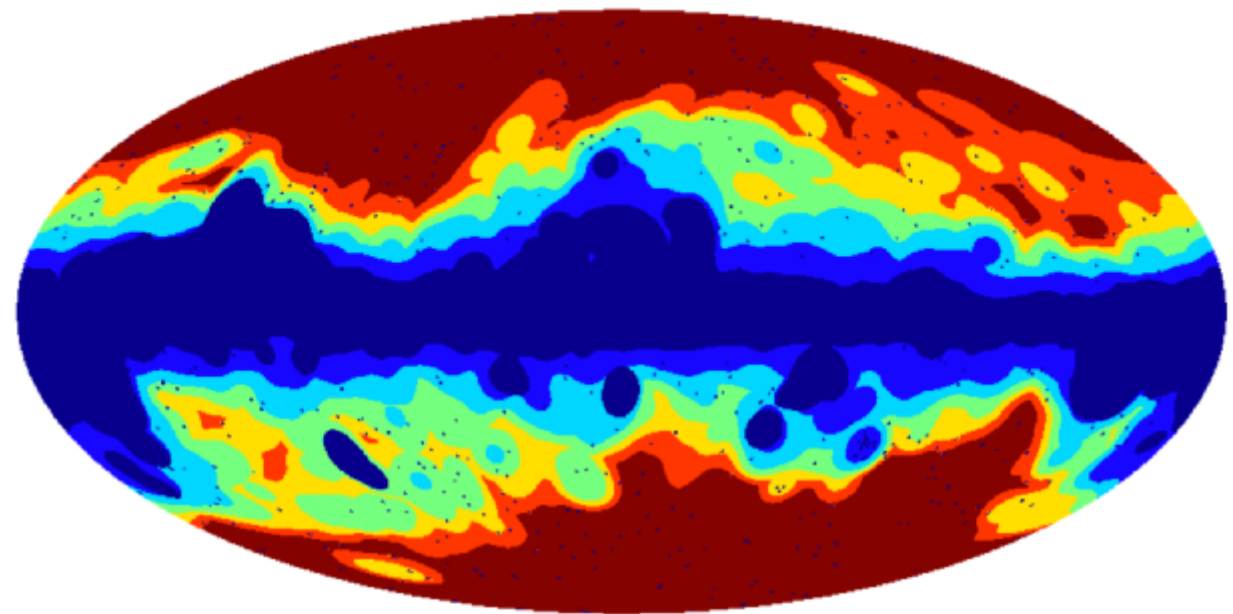
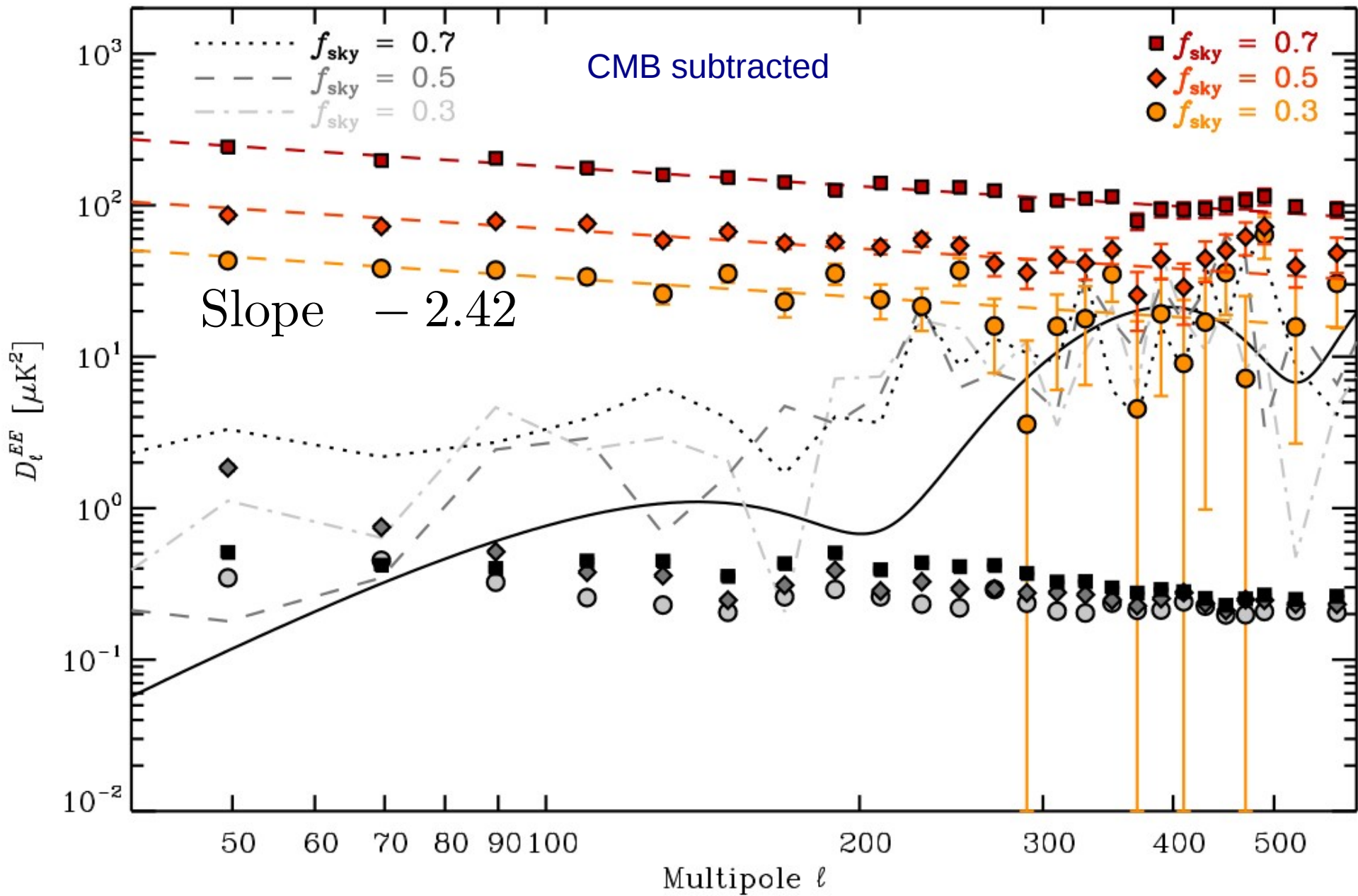


Fig. 1: Masks and complementary selected large regions that retain fractional coverage of the sky f_{sky} from 0.8 to 0.3 (see details in Sect. 3.3.1). The darkest blue is the CO mask, whose complement is a selected region with $f_{\text{sky}} = 0.8$. In increments of $f_{\text{sky}} = 0.1$, the retained regions can be identified by the colours dark red (0.3) to blue (0.8), inclusively. Also shown is the (unapodized) point source mask used.

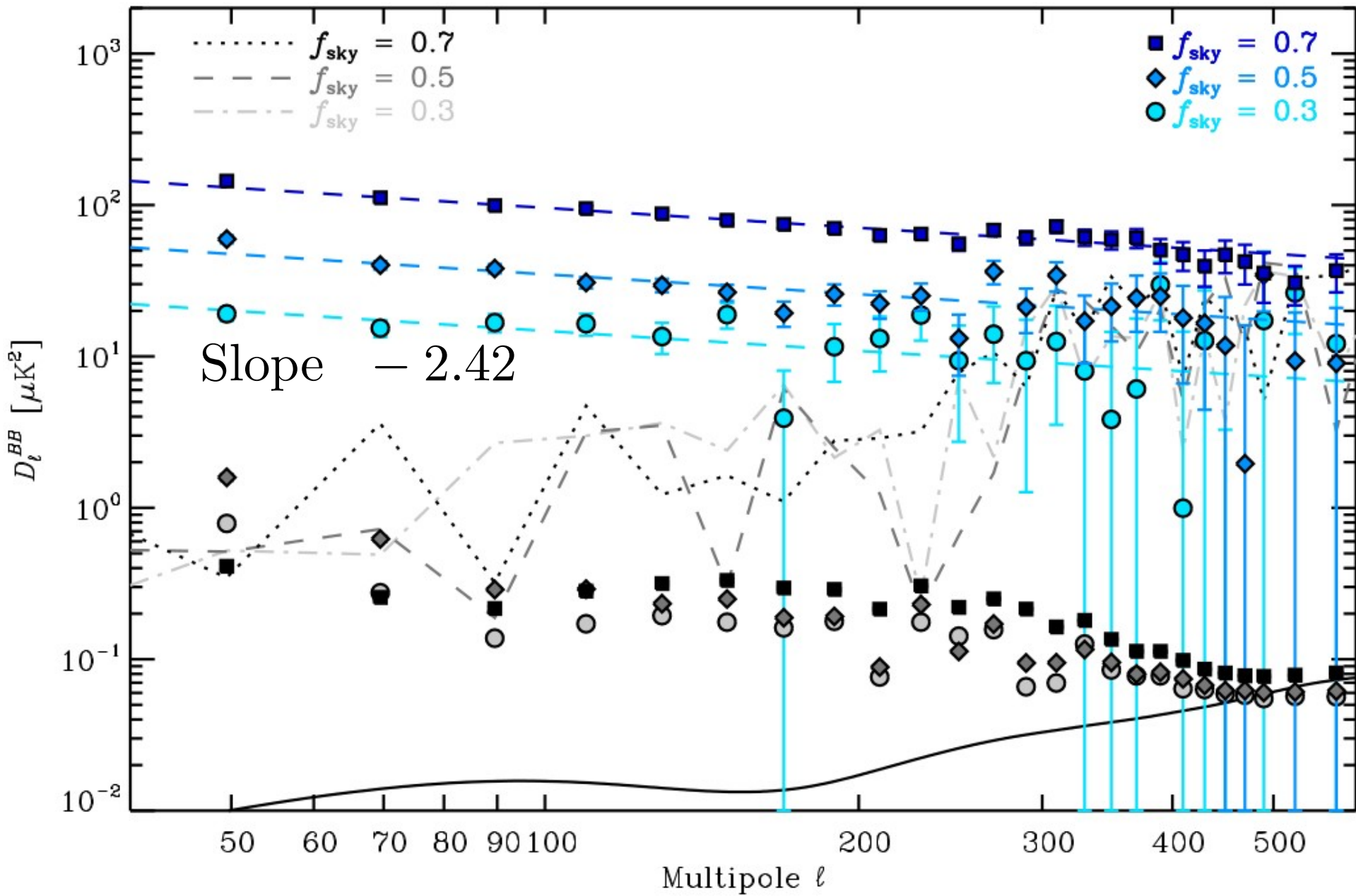
Planck analysis steps

- Detectors data (8 polarization sensitive detectors at **353 GHz**)
- Project into **Stokes parameters maps** (I, Q, U)
- Apply **mask** (10% to 80% of sky used)
- Calculate **polarization angular power spectra** (using cross power spectrum technique) for **E and B modes**
- **These are E and B modes generated by dust polarized emission in our Galaxy**
 - Nothing to do with cosmic microwave background

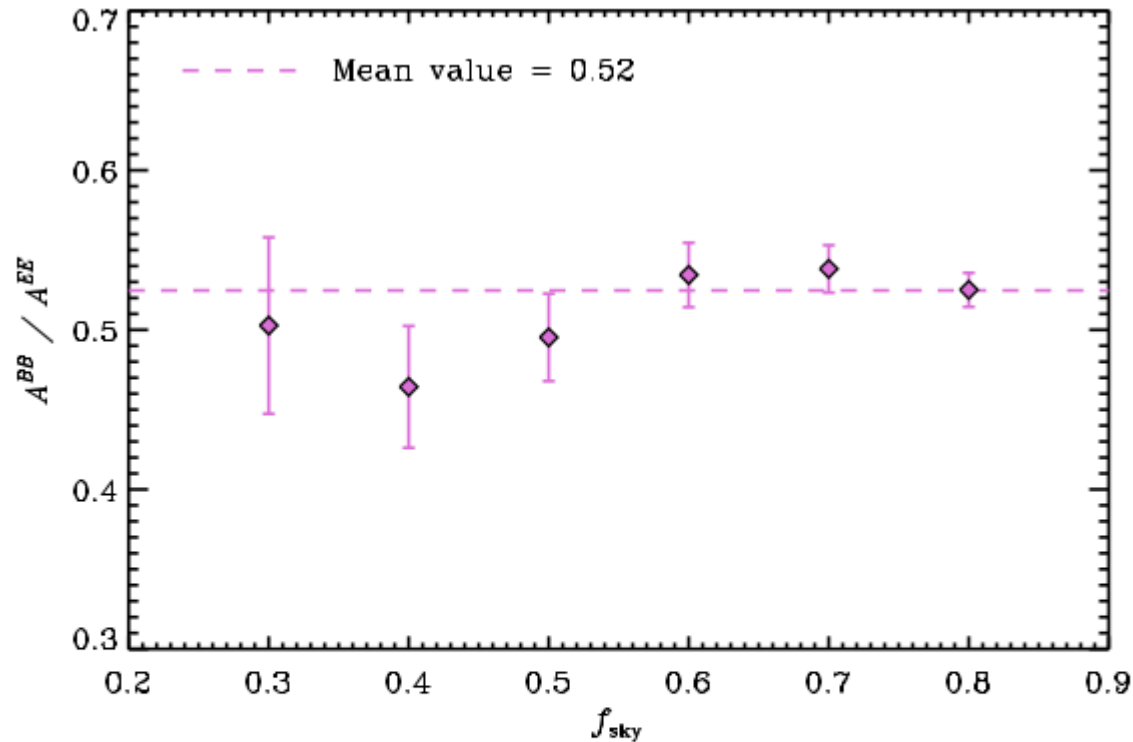
353 GHz dust E-modes



353 GHz dust B-modes



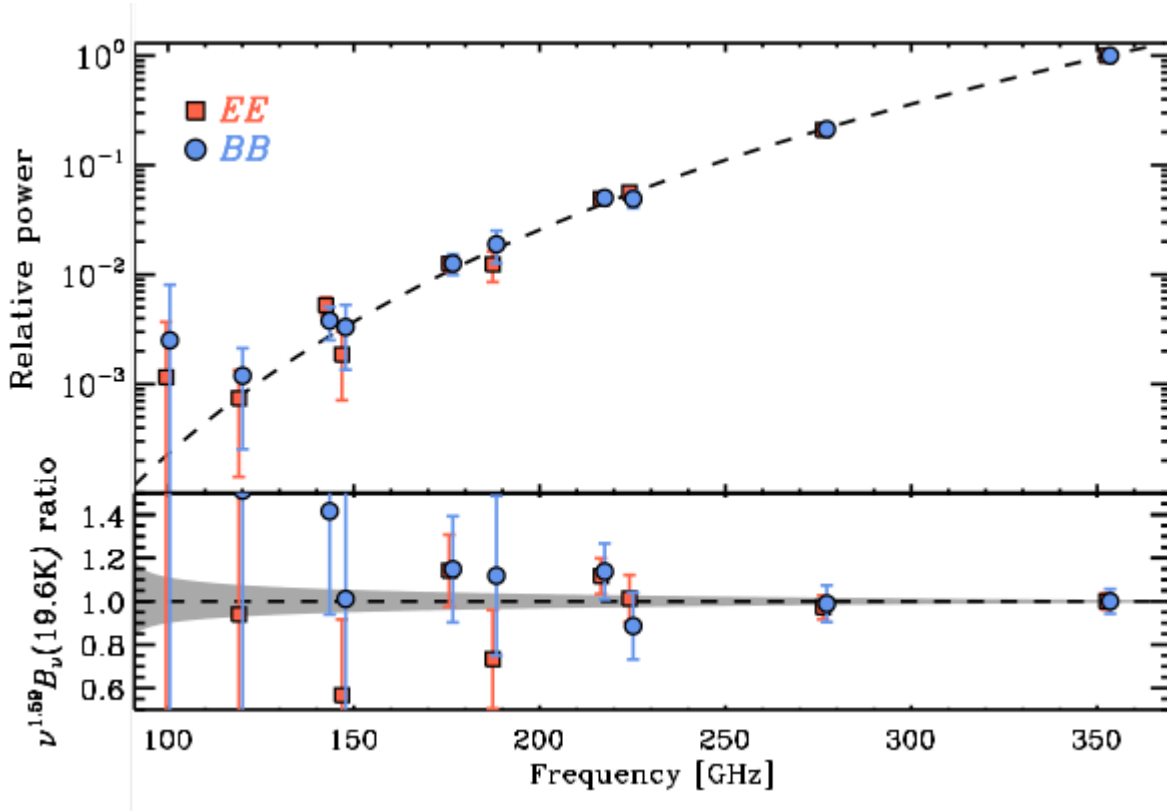
Dust B/E ratio



$$\langle A^{BB}/A^{EE} \rangle \simeq 0.5$$

Fig. 5: Ratio of the amplitudes of the \mathcal{D}_ℓ^{BB} and \mathcal{D}_ℓ^{EE} dust power spectra at 353 GHz for the different LR regions defined in Sect. 3.3.1, distinguished here with f_{sky} . The mean value $\langle A^{BB}/A^{EE} \rangle = 0.52$ is plotted as a dashed line.

Check of extrapolation law



<100x100>	<100x143>	<100x217>	<100x353>
	<143x143>	<143x217>	<143x353>
		<217x217>	<217x353>
			<353x353>

$$[Q_d, U_d] \propto \nu^{\beta_d} B_\nu(T_d)$$

$$T_d = 19.6 \text{ K}$$

$$\beta_d = 1.59 \pm 0.17$$

- Data report the amplitude of the polarization cross spectra
- The dashed curve is not a fit, it is the prediction from correlation coefficients

Analysis on large sky fraction

■ Summary

- Slope in the dust polarization angular power spectrum very regular

$$\text{Slope} = -2.42 \pm 0.02$$

- Dust B-modes are on average smaller than dust E-modes

$$\langle A^{BB} / A^{EE} \rangle \simeq 0.5$$

- Extrapolation to lower frequency is well modeled

$$\beta_d = 1.59 \pm 0.17$$



Analysis of faintest dust-contaminated regions

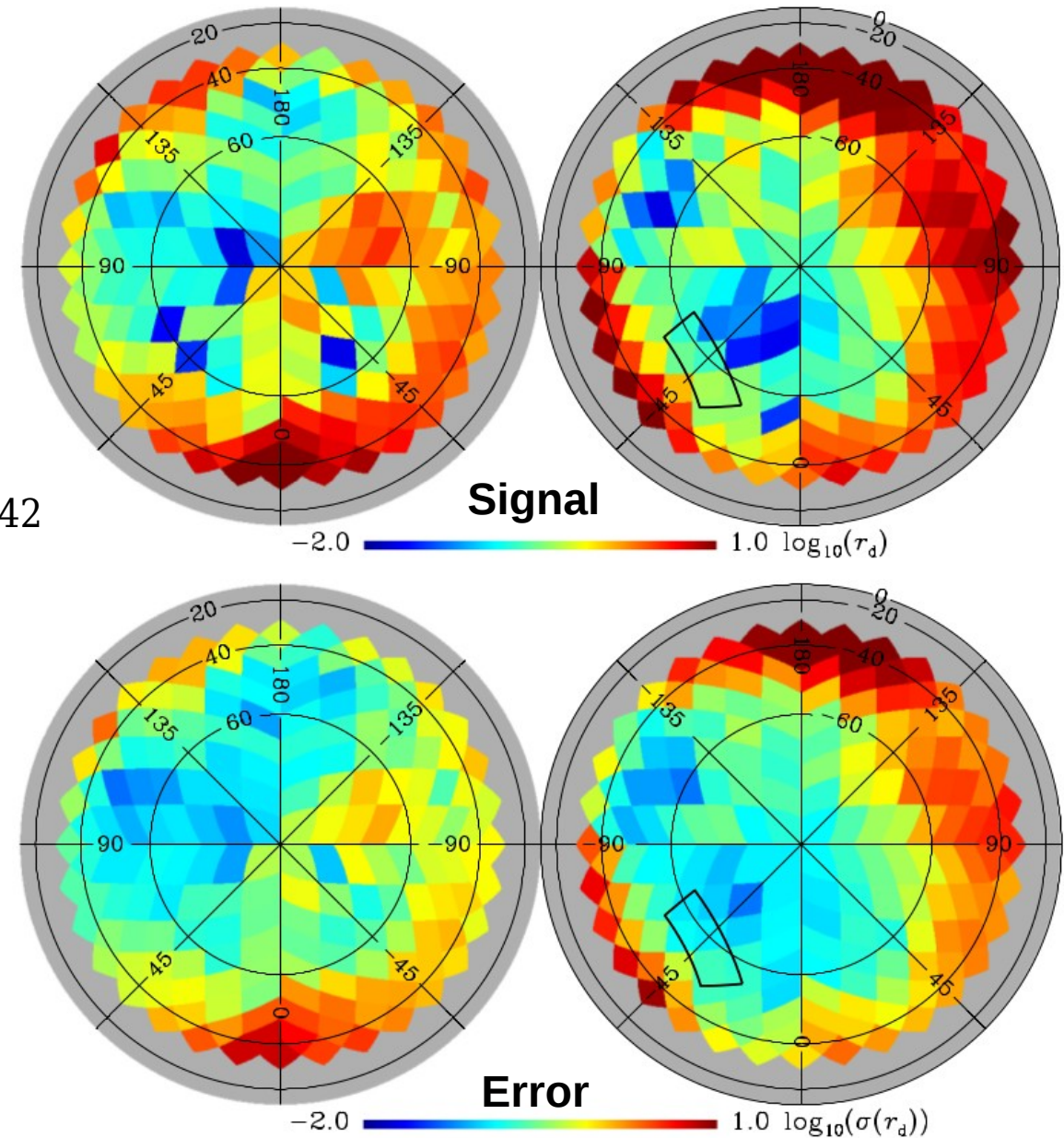
Selection of best sky patches for CMB polarization search

Search for the best sky patch

- 352 patches, 400 deg² wide
(~1% of the sky each)
- On each patch
 - Use 353 GHz polarization maps (**dust**)
 - Calculate B-modes **dust** polarization
 - Power-low fit in ell, with slope -2.42
 - Calculate amplitude value (and error) at ell=80
 - Extrapolate to 150 GHz

Search for the best sky patch

- 352 patches, 400 deg² wide (~1% of the sky each)
- On each patch
 - Use 353 GHz polarization maps (**dust**)
 - Calculate B-modes **dust** polarization
 - Power-low fit in ell, with slope -2.42
 - Calculate amplitude value (and error) at ell=80
 - Extrapolate to 150 GHz
 - Plot relative to $r=1$ case
 - Box is BICEP2 region
 - Not the best region



Analysis on faintest regions

■ Summary

- We show that even in the faintest dust-emitting regions there are no “clean” windows in the sky where primordial CMB B-mode polarization measurements could be made without subtraction of foreground emission.



Analysis in the BICEP2 field

Check of extrapolation law

- Extrapolation from 353 to 150 GHz

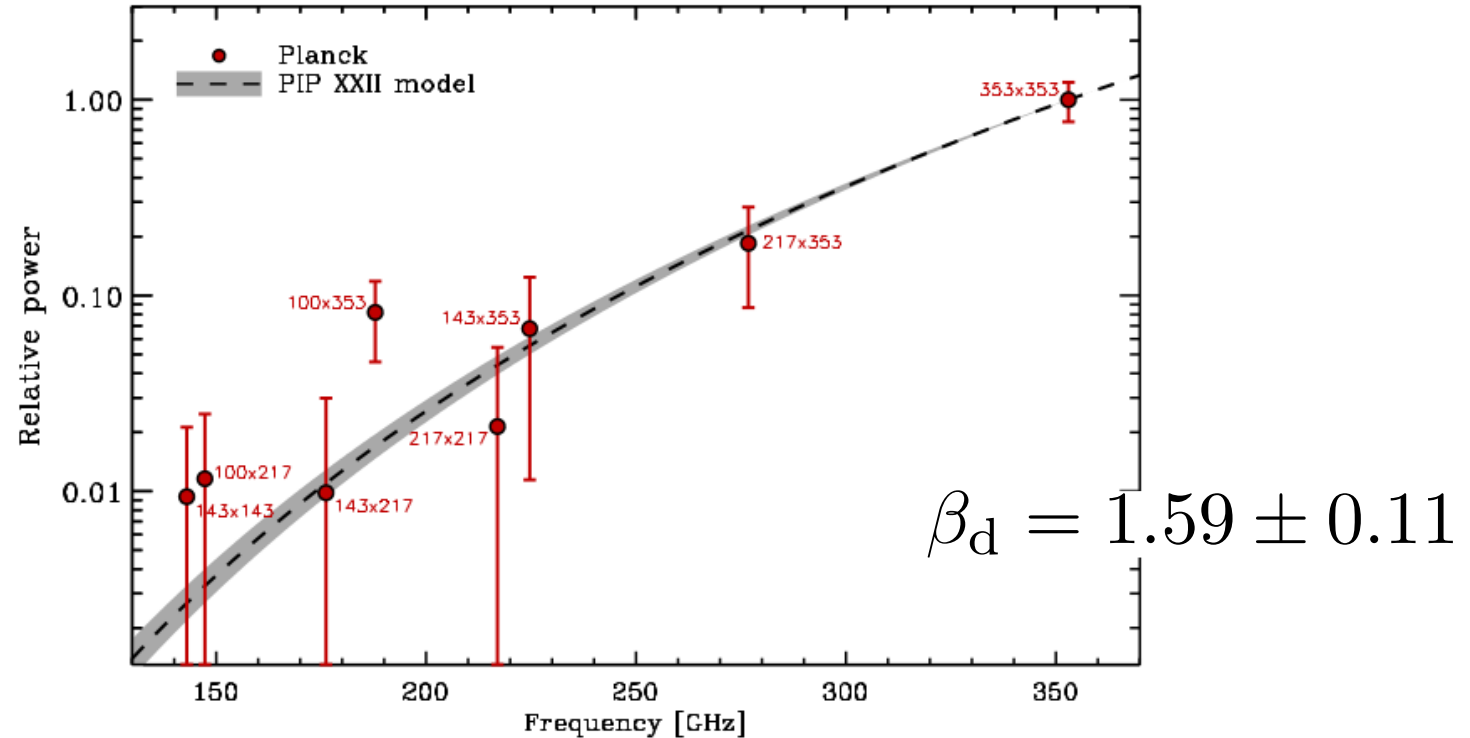
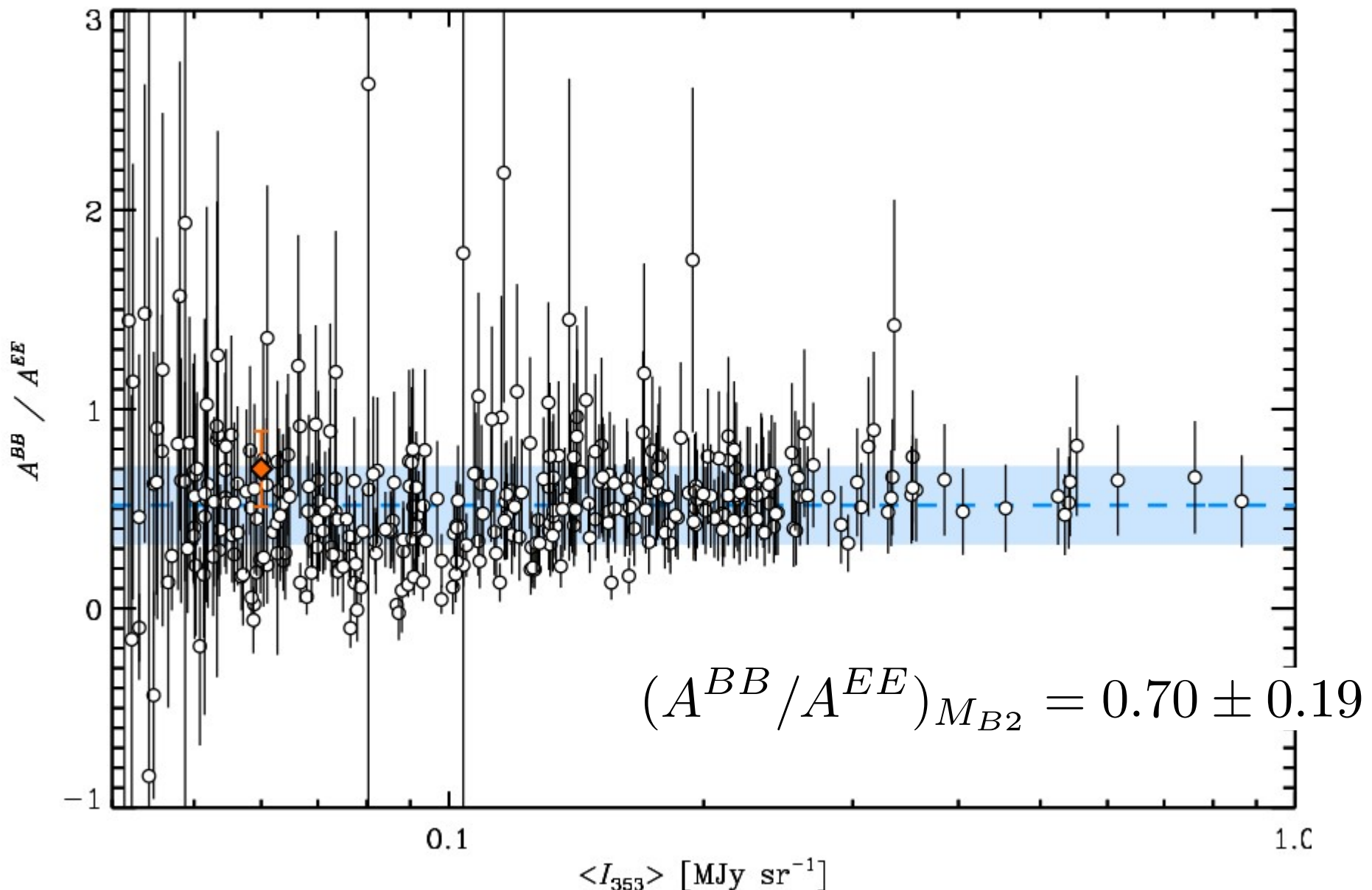


Fig. 10: Frequency dependence of the amplitude A^{BB} of the angular power spectrum \mathcal{D}_ℓ^{BB} computed on M_{B2} defined in Sect. 6.1, normalized to the 353 GHz amplitude (red points); amplitudes for cross-power spectra are plotted at the geometric mean frequency. The square of the adopted dust SED, a modified blackbody spectrum with $\beta_d = 1.59$ and $T_d = 19.6$ K, is over-plotted as a black dashed-line, again normalized to the 353 GHz point. The $\pm 1\sigma$ error area arising from the expected dispersion of β_d , 0.11 for the M_{B2} patch size (Sect. 2.2.1), is displayed in light grey.

B/E ratio



B-modes contamination

- Dust B-modes in BICEP2 field, from 353 GHz data, extrapolated to 150 GHz

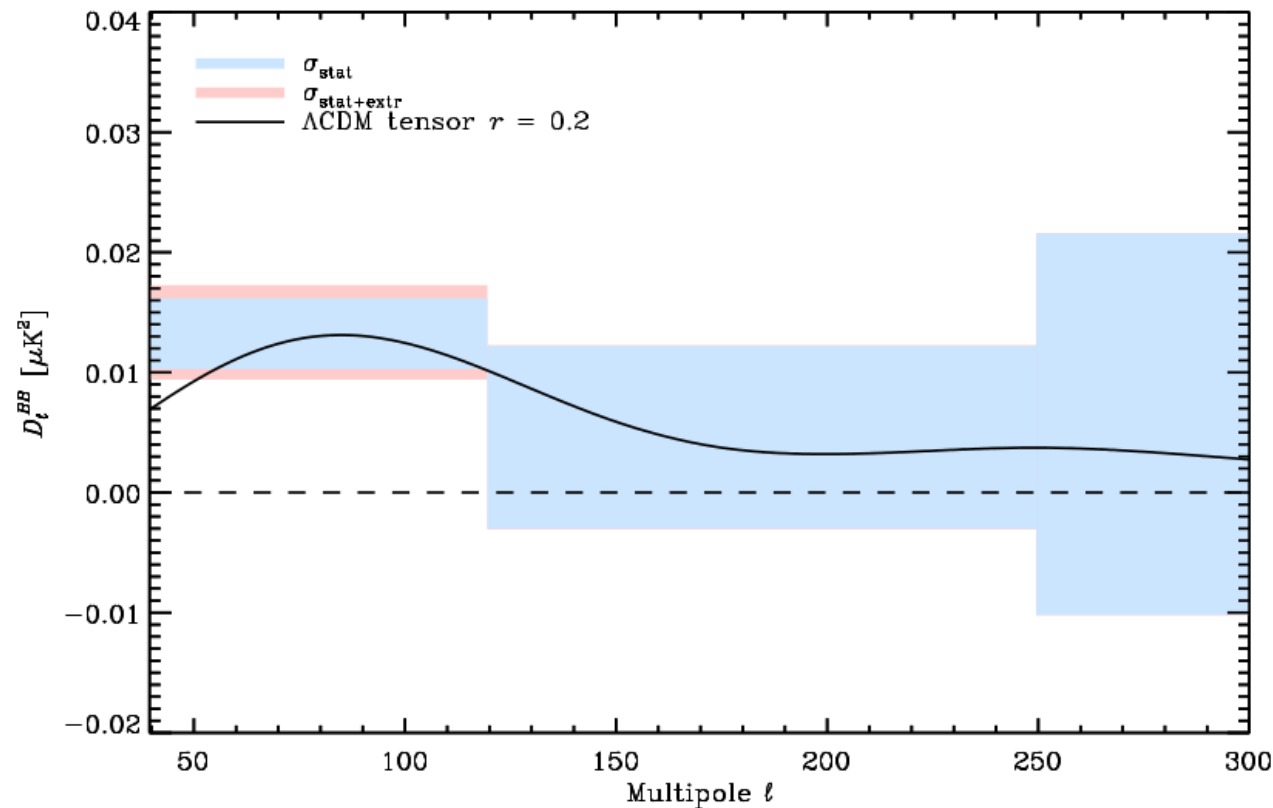
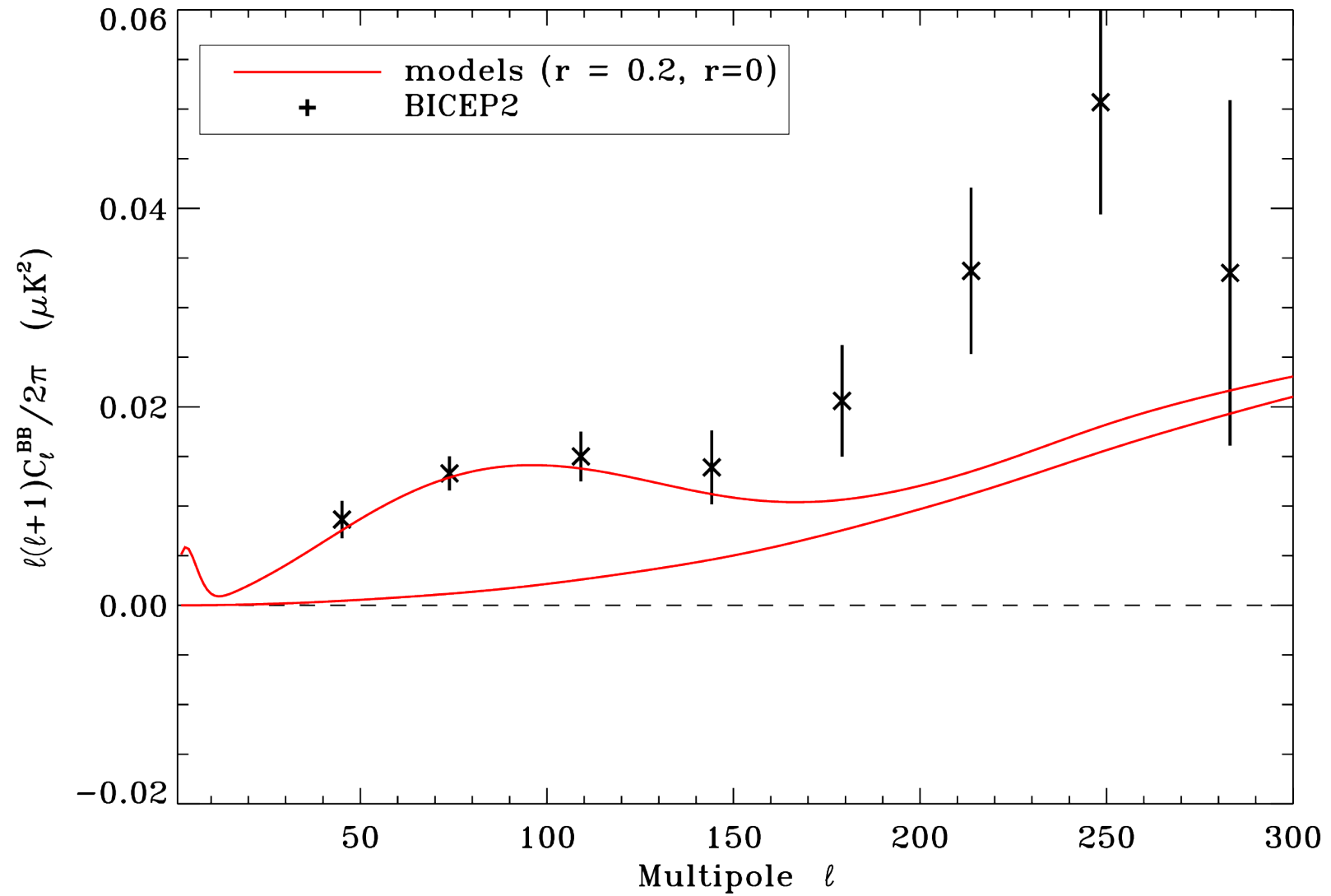


Fig. 9: Planck 353 GHz \mathcal{D}_ℓ^{BB} angular power spectrum computed on M_{B2} defined in Sect. 6.1 and extrapolated to 150 GHz (box centres). The shaded boxes represent the $\pm 1\sigma$ uncertainties: blue for the statistical uncertainties from noise; and red adding in quadrature the uncertainty from the extrapolation to 150 GHz. The Planck 2013 best-fit ΛCDM \mathcal{D}_ℓ^{BB} CMB model based on temperature anisotropies, with a tensor amplitude fixed at $r = 0.2$, is overplotted as a black line.

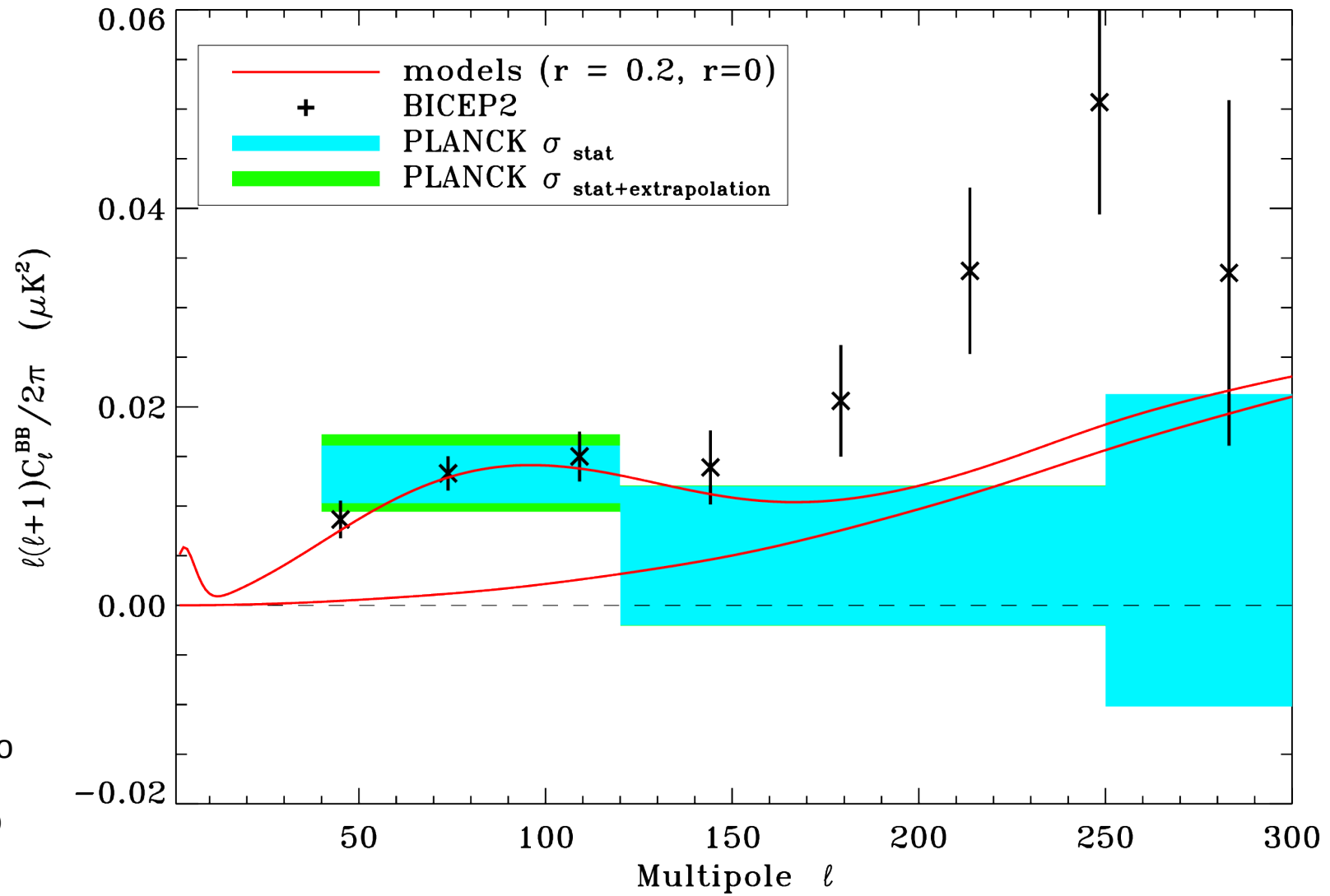
BICEP2 + models



BICEP2 + models + Planck dust



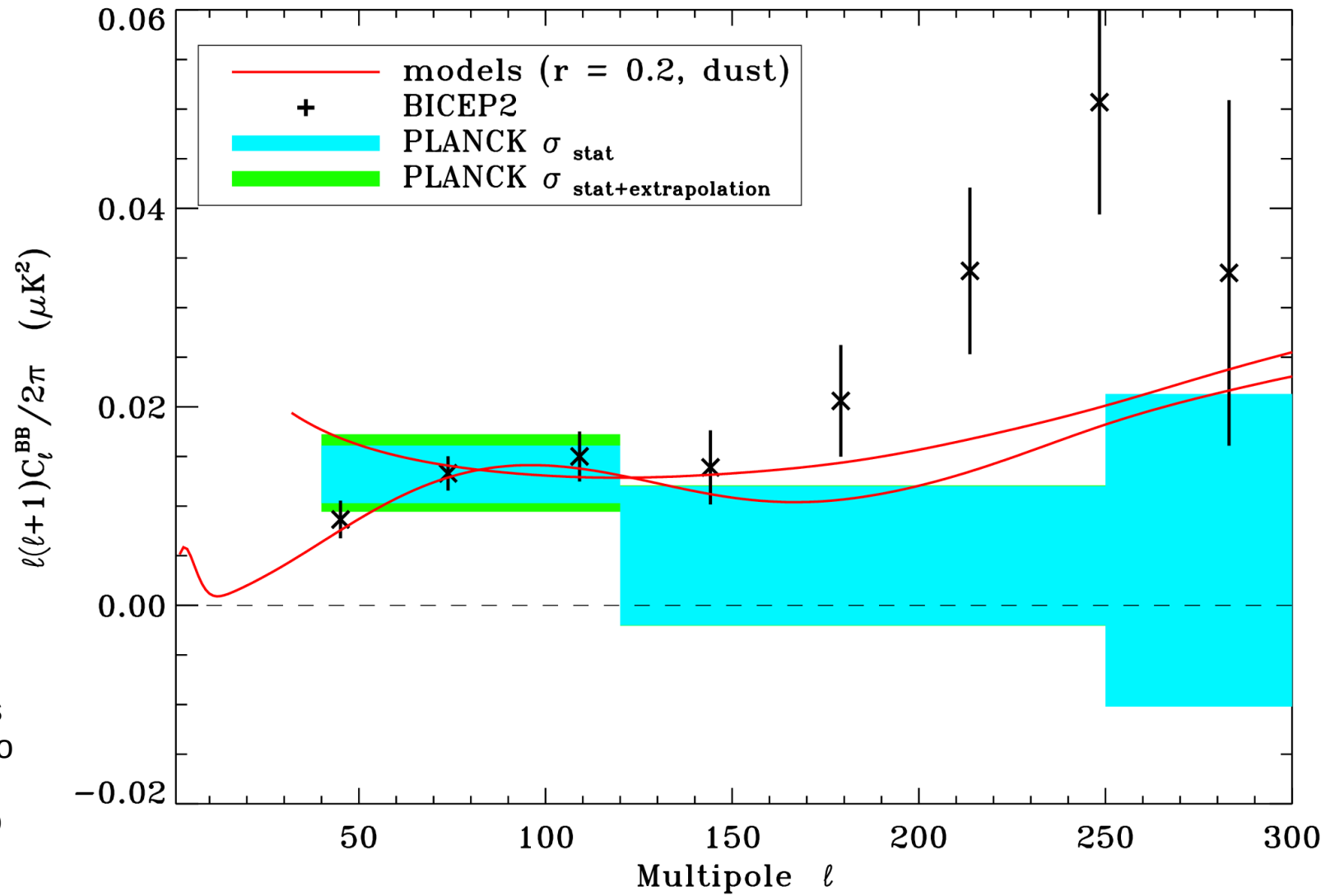
planck



BICEP2 + Planck dust + model



planck



Prospective

- Combine Planck 353 GHz data with BICEP2 150 GHz data
 - Better measure contamination
 - BICEP/Planck paper in progress
- Provide Planck own measure of the B-modes
 - Lower sensitivity
 - Larger sky fraction (highly contaminated)
 - Much better component separation
- Next generation CMB observations
 - Ground based
 - Balloon based
 - Satellite based
 - Monitoring and separation of contamination from dust and other sources is a crucial element

Comments

- Rapidly evolving science field
 - Factor 5 growth in sensitivity

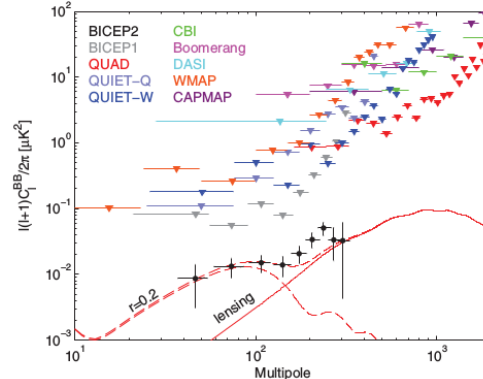
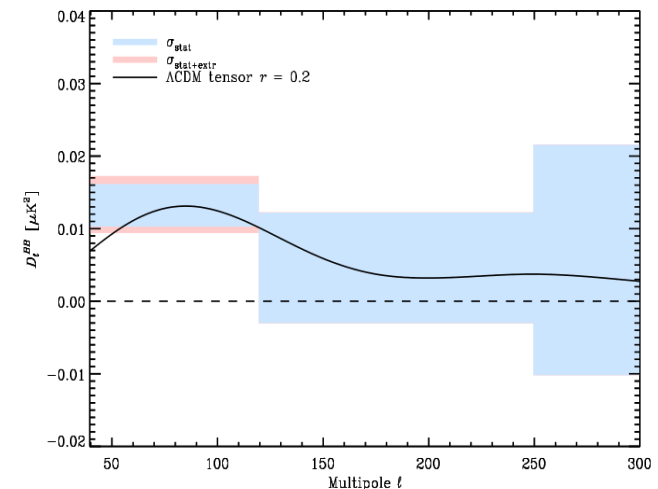


FIG. 14 (color). BICEP2 BB auto spectra and 95% upper limits from several previous experiments [2,40,42,43,47,49–51,107]. The curves show the theory expectations for $r = 0.2$ and lensed ΛCDM . The BICEP2 uncertainties include sample variance on an $r = 0.2$ contribution.

- Contamination check by a different experiment



- Combined effort: BICEP/Planck in the next months

Comments

- The inflationary paradigm still holds
 - Gravitational waves are only one of the prediction, and the level is unknown
 - Not detection of GW is not a disprove of inflation

Planck acknowledgements



planck

The scientific results presented today are the product of the Planck Collaboration, including individuals from more than 50 scientific institutes in Europe, the USA and Canada





Thank you



Intensity and polarization map

- Q, U can be decomposed in spin-2 equivalent of the spherical harmonics

$$(Q + iU)(\hat{n}) = \sum_{l,m} a_{+2,lm} {}_{+2}Y_{lm}(\hat{n})$$

$$(Q - iU)(\hat{n}) = \sum_{l,m} a_{-2,lm} {}_{-2}Y_{lm}(\hat{n})$$

- Linear combination of the coefficients

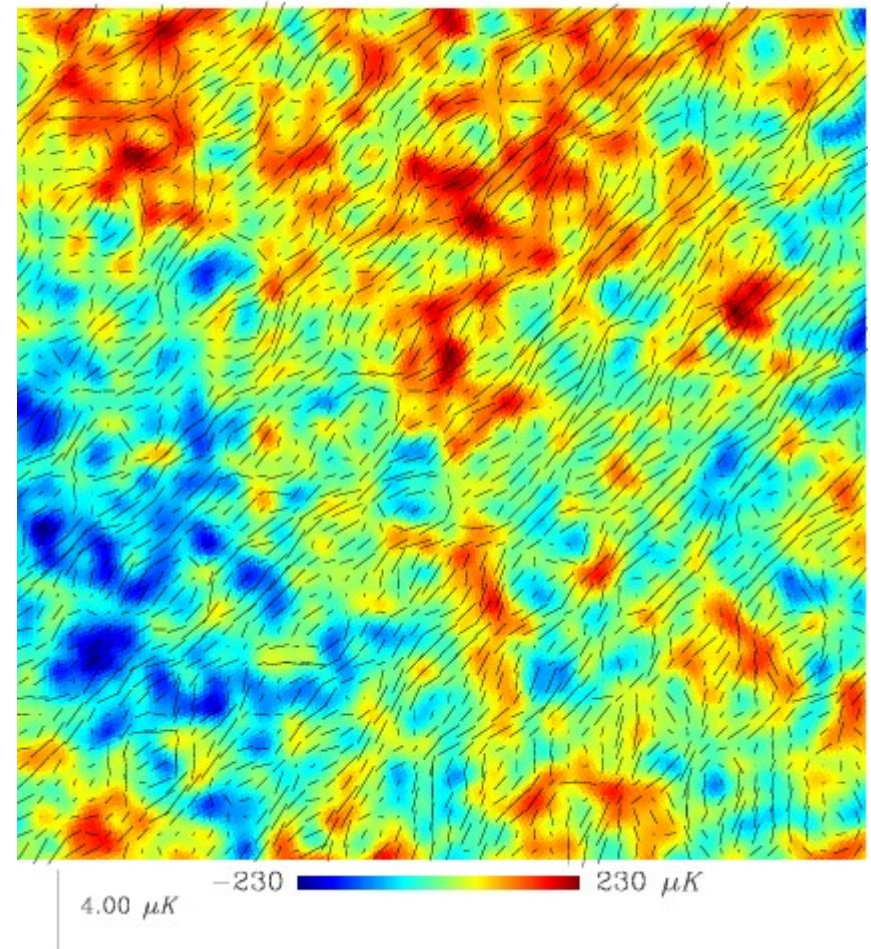
$$a_{E,lm} = -\frac{1}{2}(a_{2,lm} + a_{-2,lm})$$

$$a_{B,lm} = \frac{1}{2}i(a_{2,lm} - a_{-2,lm})$$

- Corresponds to **symmetric** and **antisymmetric** pattern decomposition

$$E(\mathbf{n}) = \sum_{\ell m} \sqrt{\frac{(\ell + 2)!}{(\ell - 2)!}} a_{E,\ell m} Y_{\ell m}(\mathbf{n})$$

$$B(\mathbf{n}) = \sum_{\ell m} \sqrt{\frac{(\ell + 2)!}{(\ell - 2)!}} a_{B,\ell m} Y_{\ell m}(\mathbf{n})$$



BICEP2 dust models

- No data, only **models**
 - Typical polarization level equal **5% of intensity**
 - Different models of the galactic magnetic field
 - **Extrapolation** with a standard trend (confirmed by Planck)
 - Planck **data revealed a higher level of dust contamination** in BICEP2 region

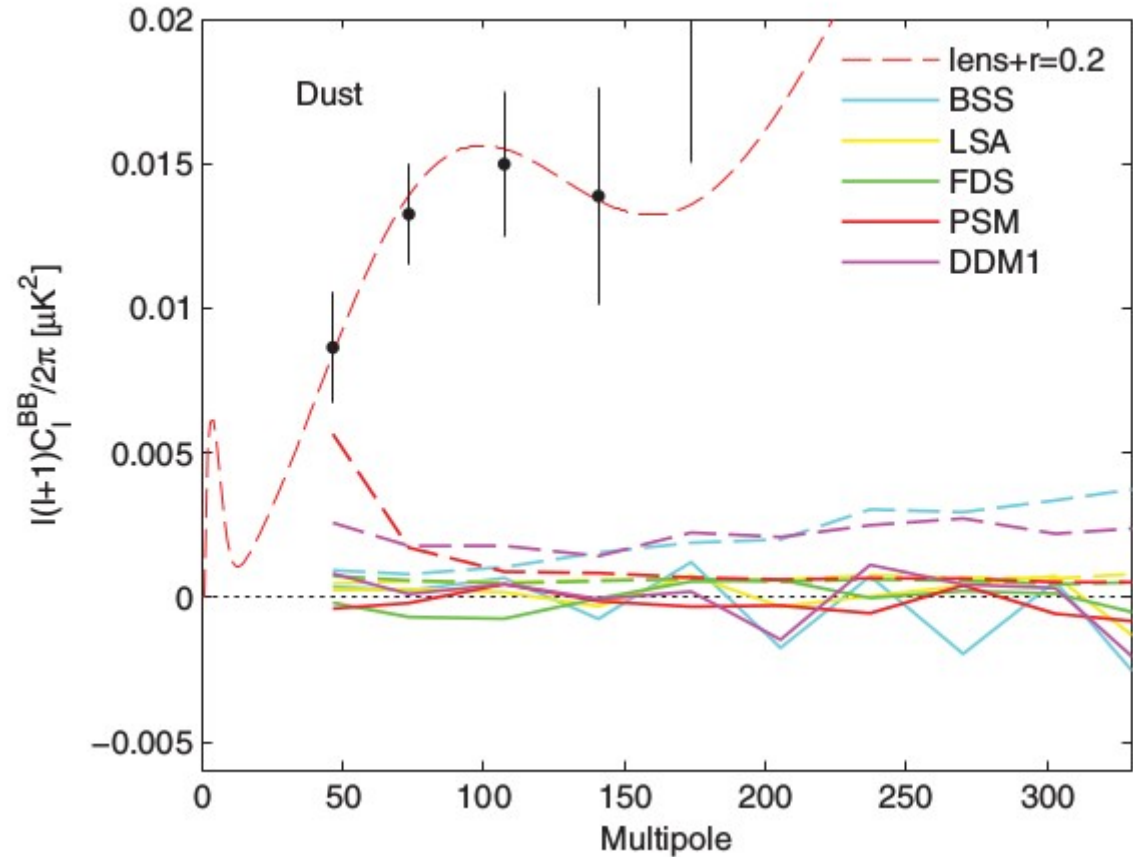
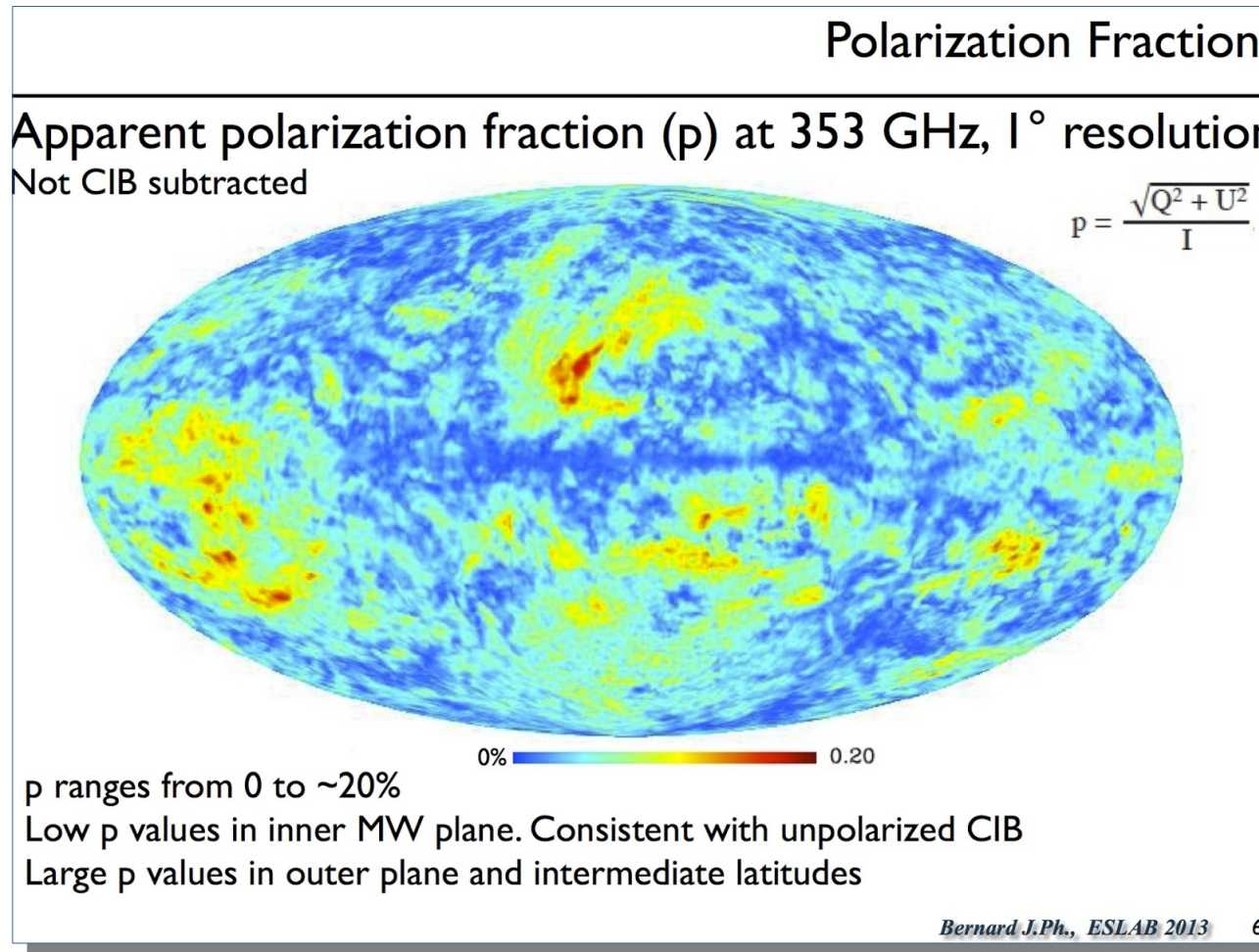


FIG. 6 (color). Upper: Polarized dust foreground projections for our field using various models available in the literature, and a new one formulated using the information officially available from *Planck*. Dashed lines show autospectra of the models, while solid lines show cross spectra between the models and the BICEP2 maps. The BICEP2 auto spectrum from Fig. 2 is also shown with the lensed- Λ CDM + $r = 0.2$ spectrum. Lower:

The removed dust model



$$p = \frac{\sqrt{Q^2 + U^2}}{I_{\text{dust}} + I_{\text{CIB}}} < \frac{\sqrt{Q^2 + U^2}}{I_{\text{dust}}}$$

Mission timeline

■ Launch	14 May 2009
■ Start of operations	14 May 2009
■ Cooldown/trip to L2	June 2009
■ Calibration and performance verification	Mid June - mid August 2009
■ First light survey	August 2009
■ Survey 1	August 2009 - February 2010
■ Survey 2	Feb 2010 - Aug 2010
■ Survey 3	Aug 2010 - Feb 2011
■ Survey 4	Feb 2011 - Aug 2011
■ Survey 5	Aug 2011 - Dec 2011
■ HFI End Of Life tests	Dec 2011 - Aug 2013
■ HFI End of Helium	13 January 2012
■ Survey 6, 7, 8 (LFI only)	Feb 2012 - Aug 2013
■ Switch-off	23 October 2013

CMB observation

The Universe is an inside-out star!

